Photochemical and microbial degradation of dissolved organic matter in the Lake Superior watershed

A THESIS
SUBMITTED TO THE FACULTY OF THE GRADUATE SCHOOL
OF THE UNIVERSITY OF MINNESOTA
BY

Megan J Macdonald

IN PARTIAL FULFILLMENT OF THE REQUIREMENTS
FOR THE DEGREE OF
MASTER OF SCIENCE

Dr. Elizabeth C. Minor

May 2012

© Megan J Macdonald 2012

Acknowledgements

Thank you to Dr. Stephanie Guildford, Dr. Josef Werne, and especially Dr. Elizabeth Minor for supporting me through my thesis project and inspiring my interest in science. Also, the guidance and encouragement of my colleagues, and the faculty and staff in the Department of Chemistry and Biochemistry were instrumental in the completion of my research. Finally, thank you to my friends and family for believing in me.

Abstract

Photodegradation of dissolved organic matter (DOM) due to ultraviolet (UV) exposure can have important consequences for coastal zone productivity. The availability of UV radiation to aquatic environments has increased due to ozone depletion. Chromophoric DOM affects the amount of light penetration in a water column. Ecosystem productivity depends in part on the input of DOM into a coastal zone. DOM can protect animals, plants, and microbes from damaging UV light by acting as sunscreen, resulting in increased ecosystem productivity. Alternatively, DOM can decrease ecosystem productivity by absorbing light needed for photosynthesis and forming reaction products that are harmful to coastal zone biota. Increased urbanization of watersheds and seasonal differences in weather patterns change the delivery pathways, reactivity, input, and energy flow of DOM into aquatic systems. Understanding the input and reactivity of DOM in coastal systems as a function of land urbanization and season will help determine the fate of irradiated organic matter and its potential role as a sunscreen in coastal waters. The consequences of energy flow from UV radiation to DOM in aquatic systems will provide useful preliminary data to be used for land-use planning in tributary regions. This study also provides data useful for predictive models of the fate of irradiated organic chemicals and the resultant impact on water quality. In this paper, the study of watershed urbanization and season on the input and photodegradation of DOM in coastal waters is discussed based on organic carbon analysis, UV-Visible spectrophotometry, microbial processing of DOM, and terrestrial (land-use) analysis.

Table of Contents

List of Tables

List of Figures

Introduction

Ozone depletion and increased urbanization of watersheds in recent years have resulted in increased availability of ultraviolet (UV) and visible radiation to aquatic environments (Arrigo, 1994; Wang et al., 2000). Colored dissolved organic matter (CDOM) can mediate the effects of such changing solar inputs by absorbing light within a water column. CDOM can increase ecosystem productivity by protecting animals, plants, and microbes from damaging UV light (Hiriart-Baer and Smith, 2005). CDOM can decrease ecosystem productivity by absorbing light needed for photosynthesis, and reacting to create harmful reactive oxygen species (Bracchini et al., 2004). Ecosystem productivity can be altered depending on which of these contrasting roles of CDOM is dominant (Amado et al., 2006). This project measures CDOM concentrations in the lower reaches of several Lake Superior tributaries during base flow and snow melt conditions, and the potential photochemical and microbial degradation of the CDOM flowing into Lake Superior from rivers in northeast Minnesota.

This study in the western Lake Superior watershed determines trends in the potential photo and microbial lability of stream-delivered CDOM. Understanding the variations in this CDOM as a function of location and season will help determine the fate of organic matter as an input to western Lake Superior, and its potential role as a sunscreen in coastal lake waters. This understanding can then better inform land-use planning in tributary regions. This study also provides a stronger foundation of data for predictive models of the fate of organic chemicals and the resultant impact on water quality

1.1 Dissolved organic matter in coastal systems

The largest reservoir of reactive organic carbon (ca. 0.6 x 10^{18}g) on Earth is contained within dissolved organic matter (DOM) in aquatic ecosystems (Hedges, 1992; Schlesinger, 1997; Kaiser and Sulzberger, 2004). DOM strongly absorbs light in the ultraviolet (UV) range, often absorbs significant quantities of photosynthetically active radiation (PAR), (Kaiser and Sulzberger, 2004) and decreases the amount of light penetration in aquatic systems (Del Vecchio and Blough, 2002). Energy flow from the exposure of coastal waters to sunlight alters both the quality and quantity of DOM (Wu et al., 2005). These changes in surface water DOM may vary depending on the source of DOM and can cause a shift in the balance of DOM enhancement versus reduction of productivity in coastal zones.

A coastal ecosystem's energy budget can have many sources and sinks, and DOM is an important component of a coastal ecosystem energy flow diagram (Figure 1). Energy flow from natural irradiation of freshwater sources to coastal systems may provide a critical link needed for understanding the impacts of DOM photodegradation.

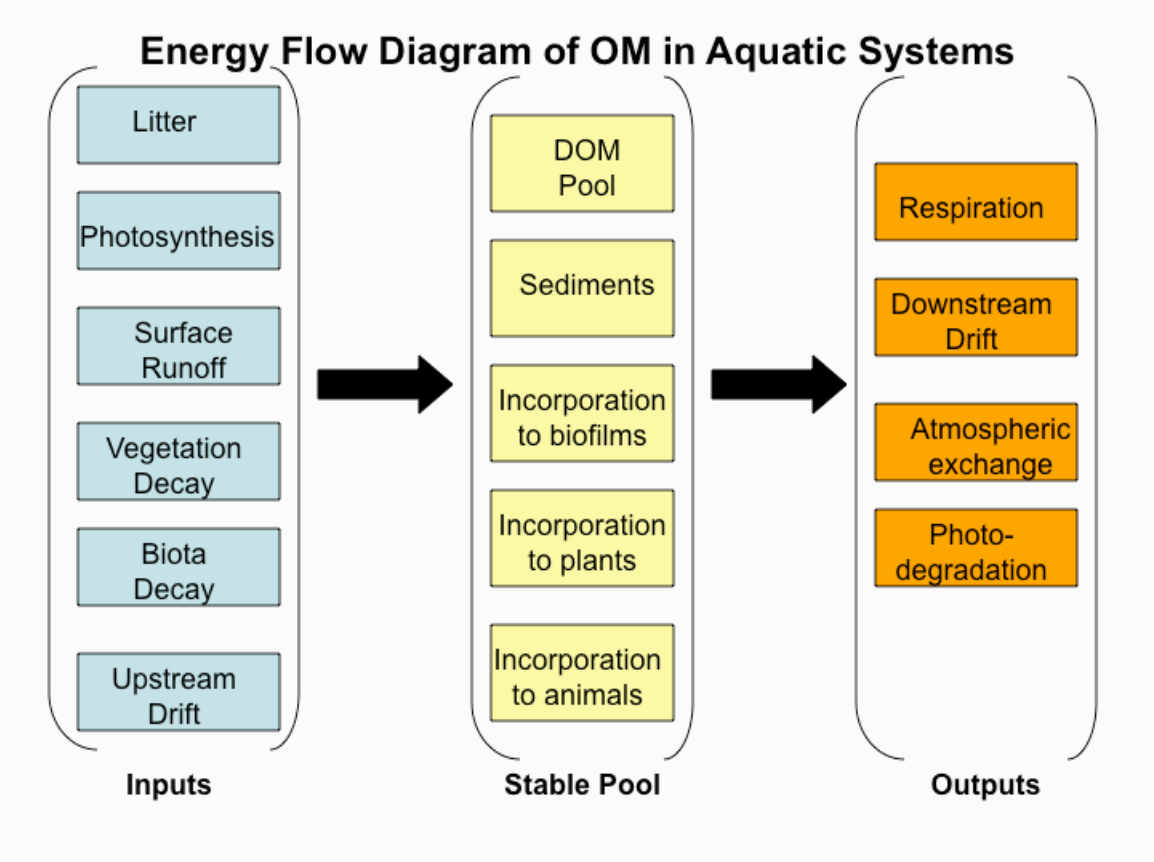

Figure 1. Proposed energy flow model in aquatic systems.

1.2 Energy transfer from Sunlight to Dissolved Organic Matter

Energy flow from sunlight to DOM can enhance coastal zone productivity by decreasing UV light exposure and reducing biota mortality (Hiriart-Baer and Smith, 2005). Additionally, photodegradation of DOM by UV radiation releases biologically available nutrients including ammonium (Bushaw et al., 1996) and orthophosphates (Francko and Heath, 1979; Zepp et al., 2011) resulting in further enhancement of coastal zone productivity. In contrast, DOM can decrease coastal zone productivity by limiting the amount of light available for photosynthesis, as well as harming biota through the photochemically-mediated release of free radicals (Bracchini et al., 2004; Zepp et al., 2011), including reactive oxygen species (Anesio et al., 2005), and toxic, bioavailable copper compounds (Zepp et al., 2011). The duration and intensity of DOM exposure to sunlight can also alter the coastal zone productivity since previous exposure reduces the ability of DOM to absorb additional UV radiation (Morris and Hargreaves 1997; Reche et al, 2001). The differences in coastal zone productivity caused by these opposing processes demonstrate the need for studies to establish how energy flow in the photodegradation of DOM changes the fate of DOM in coastal aquatic ecosystems.

Several components have already been studied with relation to the delivery and fate of photodegraded DOM in coastal aquatic systems. These include temperature, stratification, DOM and nutrient transport to surface waters, DOM production, and biological productivity (Anesio et al., 2005; Kaiser and Sulzberger, 2004; Del Vecchio and Blough, 2002; Hiriart-Baer and Smith, 2005). Table 1 and Figure 2 show the

relationship of these previously studied components to energy flow from UV radiation to DOM, and the stabilizing negative feedback loop in stable aquatic systems.

Table 1. Process cascade (1-4) controlling components of dissolved organic matter (DOM) production and photodegradation.

Component	Effect on Dissolved Organic Matter (DOM)
1. Temperature and light penetration	Increases in temperature and UV penetration lead to increased stratification and photodegradation of DOM.
2. Stratification	Increased stratification reduces the transport of DOM and nutrients to surface waters.
3. DOM and Nutrient transport to surface waters	Decreased transport of DOM and nutrients to surface waters causes a reduction in biological productivity.
4. Biological/DOM productivity	If there are sufficient nutrients, increased PAR light penetration can increase biological productivity, which can increase DOM production.

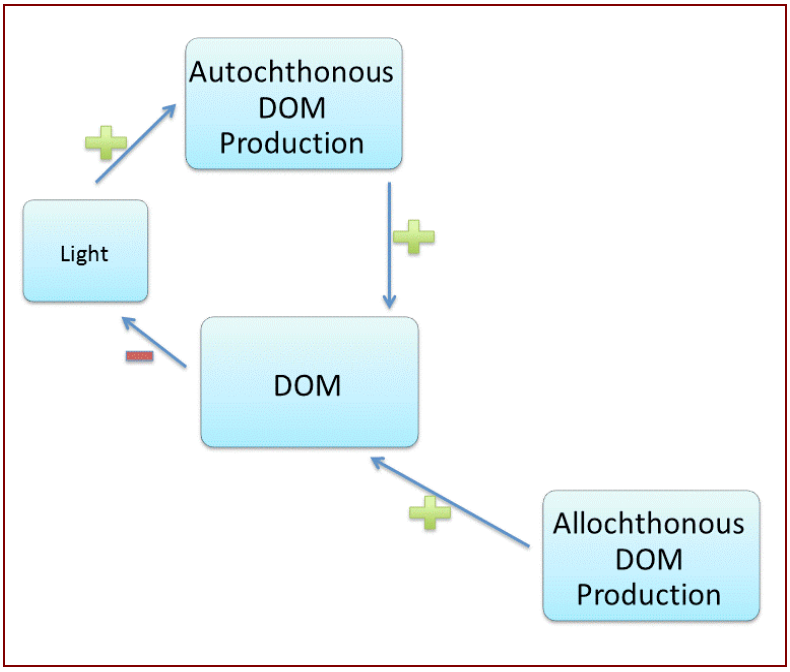

Figure 2. Stabilizing negative feedback loop of dissolved organic matter (DOM) in stable aquatic systems.

1.3 Role of Watershed Urbanization on Photodegradation of Dissolved Organic Matter

The amount and composition of DOM delivered from a stream to a coastal system is influenced by characteristics of the land use within the stream's drainage area, the watershed. Land use attributes such as population density and the presence or absence of wetlands and forests are representative components that can be used to understand the role of watershed urbanization on DOM inputs into coastal systems from streams. Aquatic DOM derived from terrestrial (allochthonous) sources is not as bioavailable as DOM produced by phytoplankton (Amon and Benner, 1996). However, photodegradation often increases the bioavailability of DOM, and increased metabolic mineralization of irradiated organic carbon in the DOM pool has been observed (Vähätalo et al., 2003).

Increased exposure of allochthonous DOM to UV radiation depending on the watershed urbanization and season of input can cause allochthonous aquatic DOM to undergo more photodegradation than autochthonous (algal and phytoplankton-derived) DOM, which is often less amenable to light adsorption due to its chemical composition and is also often quickly removed from the ecosystem by microbial processes. This suggests that photodegraded allochthonous DOM may become a more important, and perhaps more stable, energy source for coastal aquatic bacteria than autochthonous DOM. The potential increased exposure of allochthonous aquatic DOM to UV radiation compared to autochthonous aquatic DOM and the resulting changes in energy flow in aquatic systems are important factors to consider in aquatic DOM bioavailability (Vähätalo et al, 2008; Biddanda and Cotner, 2003; Larson et al., 2007).

Watershed catchments depicted through Geographic Information System (GIS) software can be used to quantify bulk land use categories including agricultural, forested, grassland, wetland, and urban (Hieb, 2005). These categories can be further generalized into urban and rural land use. Differences in photodegradation due to variation in chemical components of DOM such as aromaticity and molecular weight may be related to the land use category of a watershed. Photodegradation of riverine and coastal DOM has been established as a primary mechanism driving the variation in optical properties of offshore DOM relative to the coastal and riverine DOM (Obernosterer and Benner, 2004; Vodacek et al., 2003; Del Vecchio and Blough, 2002).

Aromaticity describes systems with delocalized π bonding resulting from conjugated carbon double bonds, lone pairs and/or empty orbitals. The aromatic components of dissolved organic matter are preferentially photodegraded in aquatic systems (Kujawinski et al., 2004; Dalzell et al., 2009). Loss of aromaticity after photodegradation may be due to preferential light absorption by and subsequent breakdown of lignin and tannin compounds. These phenolic compounds are found only in allochthonous DOM and their aromaticity is used as an identifying component for the humic fraction (Uyguner and Bekbolet, 2004) of allochthonous DOM. Photodegraded allochthonous DOM, however, is difficult to distinguish from marine-derived autochthonous DOM (Minor et al., 2007), even though these two types of DOM may originally react to UV light very differently in aquatic systems.

Previous research and data presented in this thesis show a decrease in molecular weight when DOM is exposed to natural or artificial sunlight (e.g., Dalzell et al., 2009).

A potential mechanism for this reaction is through photolysis. Upon the absorption of a photon from incoming UV radiation, aromatic compounds within organic matter undergo bond cleavage to form smaller subunits (Kieber and Mopper, 1987). This allows for increased bioavailability of the low molecular weight organic matter when the organic matter is broken down into smaller aliphatic and aromatic subunits as a result of sunlight exposure. (Granéli et al., 1996; Molot and Dillon, 1997).

Optical properties measured using UV-Visible spectrophotometry and organic carbon concentrations measured via high temperature combustion can be used to indicate molecular weight, aromaticity, and DOM concentrations.

By examining the relationship between generalized land use categories within a watershed and the concentrations and photoreactivity of aquatic DOM, a generalized understanding of photodegradation as a function of land use can begin to be established on a global scale and used for prediction. Thus, it is important to understand the photodegradation of stream DOM as a function of watershed urbanization.

1.4 Energy Flow as a Function of Watershed Urbanization

Watershed urbanization is a neglected component of aquatic ecosystem energy budgets. In low-productivity lakes in temperate regions, bacteria respire more organic carbon than can be produced by in-lake macrophytes and phytoplankton. Allochthonous input of DOM, much of this delivered by streams and rivers, acts as a supplement supporting this excess bacterial respiration (Vander Zanden and Gratton, 2011).

A study of carbon fluxes in relation to land use found dissolved inorganic carbon concentrations nearly five times greater in urban streams than forested streams (Barnes and Raymond, 2009), most likely due to respiration of organic carbon inputs to the streams. Data from an Australian watershed system shows that DOC is the principle carbon source in urban catchments (Petrone, 2010). Thus, changes to the inputs of DOC as a result of urbanization may alter the release of dissolved inorganic carbon products through respiration.

Increased urbanization of watersheds could either increase or decrease the amount of DOM available as an allochthonous input to streams and lakes. Urbanization may increase allochthonous DOM inputs to streams by providing impervious surfaces for precipitation runoff to drain DOM into streams and increasing pollutants rich in organic matter. In opposition, allochthonous DOM inputs to streams may decrease due to the removal of trees, plants, and habitable area for wildlife. Also in opposition, urbanization may increase the amount of organic matter respired within the stream reach itself (as perhaps indicated by Barnes and Raymond, 2009).

DOM may also react differently due to variations in energy flow prior to aquatic system input as a function of watershed urbanization. For example, taller plants and trees may decrease the energy flow from sunlight to the decayed leaf litter that is deposited in a natural (non-urbanized) watershed prior to stream deposition. In contrast, leaf litter deposited in an urbanized watershed could have increased exposure to ultraviolet radiation due to removal of shading from plants and trees as a result of urbanization. These variations in energy flow as a function of watershed urbanization are also susceptible to the effects of seasonal variation.

1.5 Role of Season on Photodegradation of Dissolved Organic Matter

Aquatic microbes can use allochthonous DOM as a source of energy and carbon (Köhler et al., 2002; Moran and Hodson, 1990). Photodegradation of riverine allochthonous DOM forms a series of reaction products that alter the biological reactivity of DOM photoproducts, but only some of the photoproducts are available to aquatic microbes (Moran and Zepp, 1997). As a result, energy flow from UV radiation to DOM can increase or decrease bioavailability of allochthonous DOM photoproducts to heterotrophic bacteria, and other coastal or offshore consumers of riverine DOM (Minor et al., 2007; Sulzberger and Durisch-Kaiser, 2009).

Differences in bioavailability and photoreactivity may be due to not only the origin of DOM, but also the pathway of photo-transformations. Seasonal weather changes can cause allochthonous DOM to have different levels of exposure to UV-induced photodegradation prior to riverine input. Additionally, allochthonous DOM is more available to undergo photo-transformations, whereas autochthonous DOM is more vulnerable to microbial degradation processes (Amado et al., 2006; Obernosterer et al., 2001). Furthermore, seasonal increased solar irradiation causes increased surface water temperatures. Increased surface water temperatures produce or enhance stratification of water columns. Stratification leads to a reduction in DOM mixing and more extreme photodegradation for that smaller portion of DOM trapped in the surface layer (Table 1, Figure 2). To understand these implications, seasonal variations in DOM input to coastal systems need to be investigated.

1.6 Energy Flow as a Function of Season

Seasonal changes in DOM inputs can elicit changes in the energy flow pathway from UV radiation in several ways. Allochthonous DOM deposited into streams during different seasons will undergo different reactions including photodegradation prior to input to the aquatic system. DOM from decomposed leaf litter may have chemical components with higher molecular weights and more exposure to UV radiation if the leaf litter is blown into a stream before snowfall. DOM from leaf litter that is buried under snow for several months will be blocked from sunlight but exposed to physical modification from freeze-thaw cycles, microbial breakdown, and dilution with melting snow by the time it is washed into a stream during spring snow melt. These variations in DOM inputs need to be studied to identify the role energy flow as a function of season in coastal aquatic systems.

The season of DOM input also alters the abundance of autochthonous versus allochthonous DOM present in coastal aquatic systems, and the nature of the allochthonous material (leaf-litter derived vs. woody vs. soil-derived). Seasonal control of DOM input has been documented in a mountainous region of Idaho where alpine lake processes regulate DOM concentrations across seasons (Goodman et al., 2011). Allochthonous DOM that has already been exposed to UV radiation includes dissolved organic carbon (DOC) compounds that can be utilized by bacteria. Consequently, increased photodegradation of allochthonous DOM as a result of UV radiation exposure creates degradation products that are more vulnerable to bacterial utilization and removal by photo-oxidation (Wetzel et al., 1995; Benner and Biddanda, 1998; Obernosterer et al.,

1999; Tranvik and Bertilsson, 2001).

Increases in surface water temperatures can enhance surface water concentrations of autochthonous DOM, as dissolved inorganic carbon (DIC) processing by aquatic plankton through photosynthesis is shifted toward more DOM as opposed to particulate organic matter (POM) production (Wohlers et al., 2009). The increase in DOM concentrations combined with increased UV radiation exposure and stratification of the water column may alter the energy flow pathways of aquatic systems, shifting the balance of DOM removal mechanisms between atmospheric out-gassing, sinking to sediments, and microbial biomass production. Due to seasonal influence on the photodegradation of DOM prior to aquatic system input and surface water temperatures, the energy flow from UV radiation to DOM must be studied across seasons.

1.7 Goal of Study

Figure 3 shows feedbacks (many of them underexplored areas of research) in the delivery and fate of photoreactive DOM in coastal aquatic systems. The study approach described in this paper provides a preliminary data set showing the influence of watershed urbanization and seasonal variations on the photodegradation of DOM. For an initial scaling of photochemical modifications to DOM relative to microbial modifications, a replicate set of base-flow samples from June 2010 were exposed to short-term microbial degradation after inoculation with Lake Superior whole water samples.

Understanding urbanization and season as moderators of energy flow in aquatic systems will provide insight as to how tributary region restoration can be used to minimize negative impacts of DOM changes in coastal aquatic systems.

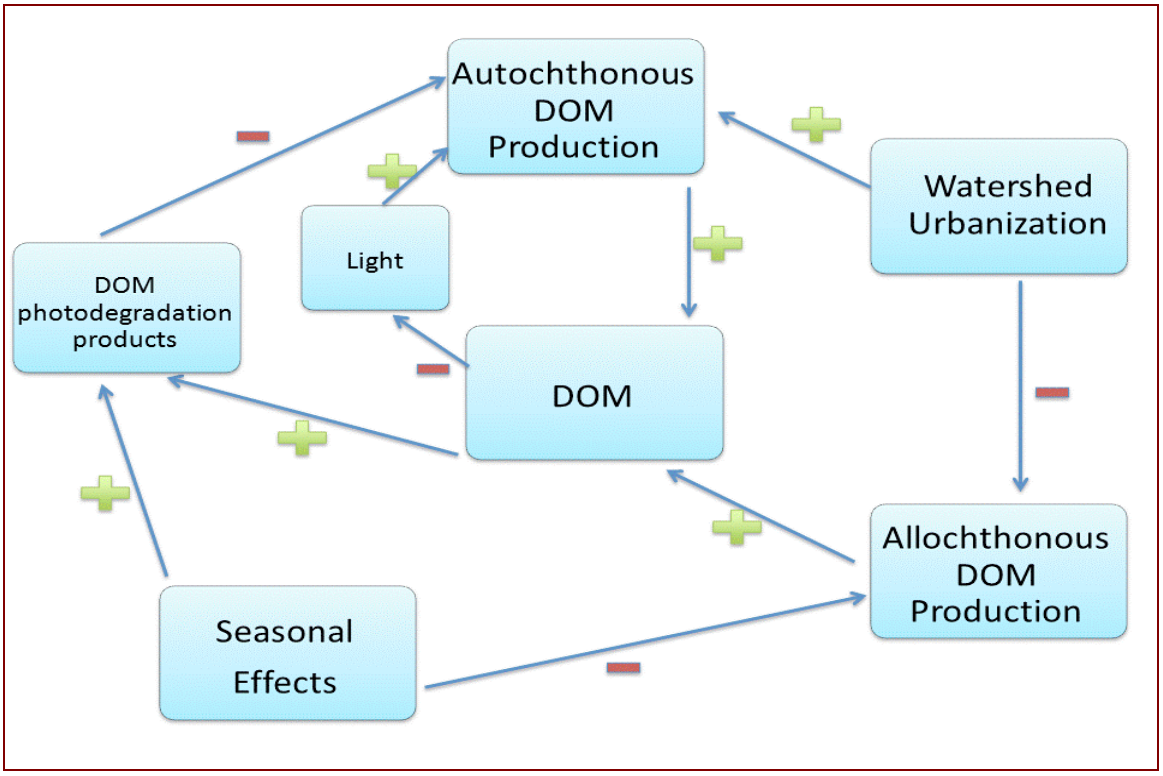

Figure 3. Model of study to determine the role of watershed urbanization and season on the input and fate of photodegraded DOM. Green plus signs indicate positive effects, and red dashes indicate negative effects. The dominance of positive or negative effects of season and watershed urbanization is to be determined experimentally.

2. Sampling & Methods

2.1 Sampling locations

Water samples were collected between June 2010 and March 2011 from five Minnesota designated trout streams in the western Lake Superior watershed (Figure 4). Criteria required in the state of Minnesota to add a stream to the Designated Trout Stream List include the following: water temperature must be less than 72 degrees Fahrenheit when air temperature is greater than 80 degrees Fahrenheit; the concentration of oxygen must be greater than five parts per million; and an area hydrologist must verify the presence of definable bed and banks in the stream (Minnesota Department of Natural Resources, 2011). The presence of trout is not required for designation as a trout stream.

Trout stream sampling locations included near the shore of Lake Superior at Amity Creek (46.839019 N, -92.007086 W), French River (46.89937 N, -91.892245 W), Gooseberry River (47.14585 N, -91.454294 W), Kingsbury Creek (46.724437 N, -92.189949 W), and Miller Creek (46.764608 N, -92.133172 W).

Amity Creek (Am) is located at the east end of the City of Duluth. Although it is located within the city limits, Amity Creek's watershed is only 2% urban (LakeSuperiorStreams, 2009; Figure 2). The French River (F) is located east of Amity Creek and has a steeper slope than the steams sampled to the west. The French River watershed is 1% urban. The Gooseberry River (Gb) was sampled at a location just below the three waterfalls before flow into Lake Superior. The Gooseberry River is located within a state park east of the French River and its watershed is less than 1% urban. Kingsbury Creek (K) is located west of Amity Creek in the city limits of Duluth. It

travels through the Lake Superior Zoo, and the Kingsbury Creek watershed is 18% urban. Miller Creek (M) is located west of Kingsbury Creek. It has a highly impacted watershed due to the abundance of impervious surfaces and shallow depths. The Miller Creek watershed is 39% urban.

In this study relationships between stream locations, the land use within each stream's watershed, total organic carbon (TOC) and dissolved organic carbon (DOC) concentrations, and DOM absorbance proxies were investigated. The potential links between these and photodegradation were also explored.

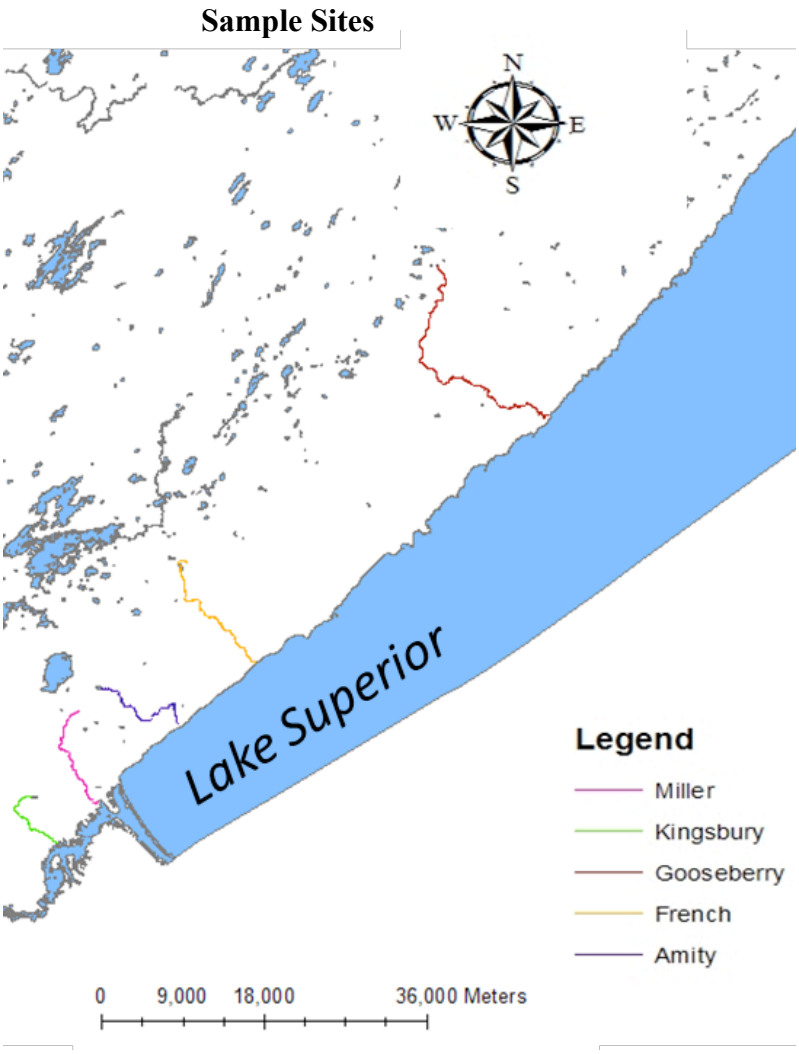

Figure 4. Stream site locations from West to East: Kingsbury Creek, Miller Creek, Amity Creek, French River, and Gooseberry River.

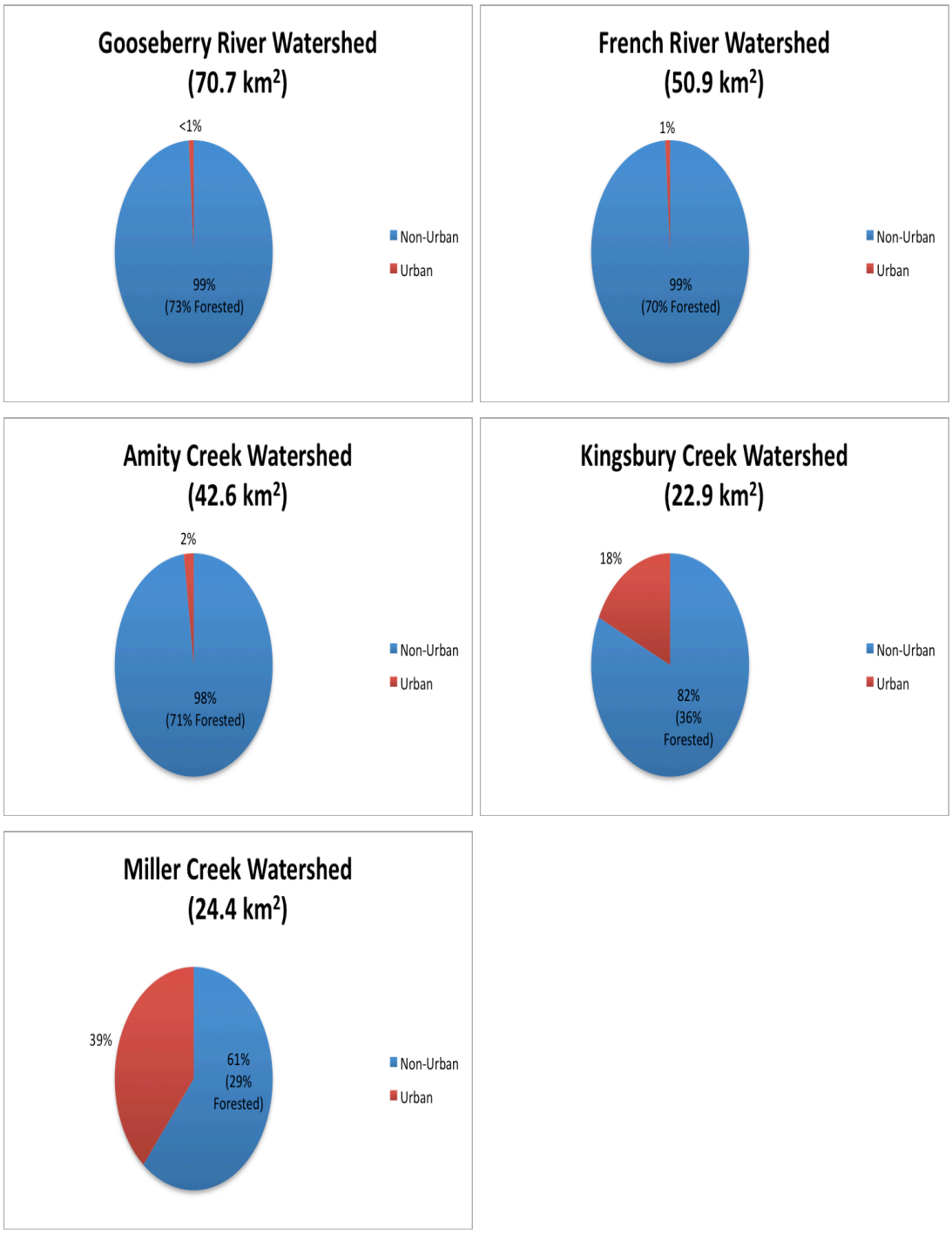

Figure 5. Watershed land use summary of the five sites studied. Within the pie charts, forested numbers (in parentheses) are percentages relative to the entire watershed. Data accessed on July 5, 2011 from http://www.lakesuperiorstreams.org/streams/landuse/landuse.html.

2.2 Sample Collections

All sampling sites were accessible by land and samples were collected in acid-washed polypropylene carboys. Each site was located near the stream input into Lake Superior. The maximum and minimum distance from stream sample collection site to Lake Superior was 914 m and 44 m for Miller Creek and the French River, respectively. The locations of all sample collection sites and each stream's entry point into Lake Superior are shown in Table 2.

Carboys and caps were rinsed with sample three times immediately prior to collection. Samples were transported back to the laboratory within two hours of sample collection. Unfiltered whole water aliquots of sample were collected for organic carbon (OC) analysis using high temperature combustion, UV-Visible absorption spectrophotometry (UV-Vis), and bacterial enumeration via epi-fluorescence microscopy.

Table 2. Latitude and longitude of sample collection sites and corresponding Lake Superior confluence points, as well as distance calculated by the Vincenty ellipsoidal formula for geodetic distance.

	Latitude (Sample Site)	**Longitude (Sample Site)**	**Latitude (Lake Superior)**	**Longitude (Lake Superior)**	**Distance**
Gooseberry River (Gb)	47.14585°N	91.454294°W	47.145325°N	91.453393°W	90m
French River (F)	46.89937°N	91.892245°W	46.899136°N	91.891773°W	44m
Amity Creek (Am)	46.839019°N	92.007086°W	46.836259°N	92.005799°W	322m
Kingsbury Creek (K)	46.724437°N	92.189949°W	46.722848°N	92.182353°W	607m
Miller Creek (M)	46.764608°N	92.133172°W	46.763432°N	92.121327°W	914m

2.3 Sample Seasons

Samples were collected to compare the effect of sample season on TOC and DOC concentration, color, photodegradability, and microbial degradability. The two sample seasons used for comparison include base flow and snow melt.

Base flow conditions represent the natural stream discharge during dry conditions (i.e., not affected by rain events, ice out, or snow melt). Base flow samples were collected during June, July, and August 2010. Prior to each sample site collection, Amity Creek was checked as a reference site of current conditions to determine if the stage height and flow rate reflected base flow conditions. Amity Creek data (LakeSuperiorStreams) was posted from a Minnesota Pollution Control Agency (MPCA) ultrasonic distance sensor. It measured water levels continuously at a frequency of 1 Hz and averaged the data every 10 seconds. Stage height data was used to calculate flow from a U.S. Geological Survey rating curve.

The snow melt sampling season was represented by samples from March 2011 collected immediately following ice melt on the streams. These conditions reflect very high flow with increases in runoff and DOM transport, as over ground flow transports more terrestrial OM than ground water flow. Stream monitors had been removed for the winter and were not available at the time of snow melt collection, so samples from all streams were collected as soon as ice had melted off the streams rather than after checking gage data. Although stage height and flow were not measured at the time of snow melt sample collection, water flow was observed to be very high during snow melt

sample collections in comparison to flow observed during base flow sample collections and storm events.

2.4 Sample Processing

a. Filtration procedure

Filtrations on 0.7μm pore size glass fiber filters (GFF, Whatman) and 0.22μm pore size membrane filters (Millipore Durapore GVWP) were performed using a pre-combusted (450°C for 4 hours) side arm flask connected to a vacuum hand pump. Glass fiber filters were pre-combusted and the filter was changed after a maximum volume of 500mL filtrate had passed through the filter. Membrane filters were rinsed with a 10mL filtration of Milli-Q water followed by 5mL sample filtration over a waste flask to prepare the disc prior to collection of filtered DOM samples. After setup on a clean pre-combusted side arm flask, new membrane filters were used for every 250mL of sample.

b. Base Flow Samples

Two sets of base flow samples were collected. Aliquots of base flow samples processed directly from the collection flask were named "whole". The remaining whole samples were filtered through 0.7μm pore size glass fiber filters (GFF, Whatman), and then the GFF filtrates were filtered through 0.22μm pore size membrane filters (Millipore Durapore GVWP). The resulting <0.22μm filtered samples were named "init" and were stored at 4°C in dark bottles for up to 52 days (Table 2). Samples analyzed after removal from refrigeration but before exposure to sunlight were named "start". All "start" samples were placed in a water bath in natural sunlight for approximately six hours. The samples that were exposed to natural sunlight in quartz flasks were named "exp". The samples

that were exposed to the same conditions as “exp” samples but were blocked from sunlight exposure in borosilicate flasks wrapped in aluminum foil were named “control”.

c. Snow Melt Samples

One set of snow melt samples was collected. Unfiltered samples were named “whole.” Aliquots of whole samples were then GFF and 0.22μm membrane filtered to form the “init” samples. “Init” samples were stored in the refrigerator for up to 120 days. Half of the volume of the “init” samples (approximately 500mL) was removed from refrigeration and re-filtered through GFF and then 0.22μm membrane filters to form the “start” samples. Remaining “init” sample was returned to the refrigerator. “Start” samples were exposed to natural sunlight in a water bath for approximately six hours. Samples exposed to sunlight in quartz flasks were named “exp”, while samples blocked from sunlight with foil-wrapped borosilicate flasks were named “control”. This portion of irradiations was collectively referred to as snow melt 1 (SM1).

Fifteen days later, the remaining half of the volumes of the “init” samples were removed from refrigeration, re-filtered on GFF and then 0.22μm membrane filters to form the “start” samples. “Start” samples were exposed to natural sunlight for approximately six hours, with exposed samples named “exp” and foil-wrapped samples named “control”. This portion of irradiations was collectively referred to as snow melt 2 (SM2).

Table 3. Dates of sample collection, sample irradiation, and the number of days that "init" samples were stored in the lab refrigerator prior to irradiation.

Base flow			
Sample	*Collected*	*Irradiated*	*Days stored*
Gb June	18-Jun-10	9-Aug-10	52
Am June	21-Jun-10	29-Jun-10	8
F June	21-Jun-10	29-Jun-10	8
K June	1-Jul-10	22-Aug-10	52
M June	1-Jul-10	22-Aug-10	52
Gb July	13-Jul-10	9-Aug-10	27
Gb August	6-Aug-10	22-Aug-10	16
K August	26-Aug-10	29-Aug-10	3
M August	27-Aug-10	29-Aug-10	2
F August	28-Aug-10	29-Aug-10	1
Am August	28-Aug-10	29-Aug-10	1
Snow Melt 1			
Sample	*Collected*	*Irradiated*	*Days stored*
SM1 F	16-Mar-11	28-Jun-11	104
SM1 K	19-Mar-11	28-Jun-11	101
SM1 M	19-Mar-11	28-Jun-11	101
SM1 Am	28-Mar-11	28-Jun-11	92
SM1 Gb	28-Mar-11	28-Jun-11	92
Snow Melt 2			
Sample	*Collected*	*Irradiated*	*Days stored*
SM2 F	16-Mar-11	13-Jul-11	119
SM2 K	19-Mar-11	13-Jul-11	116
SM2 M	19-Mar-11	13-Jul-11	116
SM2 Am	28-Mar-11	13-Jul-11	107
SM2 Gb	28-Mar-11	13-Jul-11	107

2.5 Organic Carbon Analysis

Samples collected for organic carbon analysis were acidified to pH 2 using Certified ACS Plus grade HCl (Fisher Chemical) for removal of inorganic carbon. After acidification, samples were stored at 4°C in amber glass vials until analysis on a high temperature combustion total organic carbon analyzer (Shimadzu TOC_{VSH}) coupled with an autosampler at the University of Minnesota Duluth (Figure 6). All organic samples were measured as non-purgeable organic carbon (NPOC). Standardization was provided by potassium hydrogen phthalate samples. Calibration curves were made for each NPOC analysis using a minimum of six potassium hydrogen phthalate standards of varying concentrations. Milli-Q blank samples were included throughout the analysis sequence to assess instrumental performance. Prior to sample analysis, each sample was sparged for three minutes and thirty seconds to purge inorganic carbon from the acidified samples. Each sample had a minimum of three replicate injections to ensure a coefficient of variation (CV) below 2%. All sample concentrations were calculated as the average of the three samples with the lowest standard deviation.

Figure 6. Shimadzu TOC_{VSH} coupled with an autosampler at the University of Minnesota Duluth.

2.6 UV-Visible Absorption Spectrophotometry

UV-Vis spectra were collected on a Varian Cary50 Bio spectrophotometer located at the University of Minnesota Duluth. The instrument utilized a xenon flash lamp with a bandpass of 1.5 nm. Absorbance and transmittance values were set to a reproducibility of 0.1 nm and wavelength accuracy of ± 0.5 nm at 541.94 nm (Agilent calibrated using NIST 930D filters). Samples were analyzed in a 10mm quartz cuvette (Fischer Scientific, model 14-385-902C).

The cuvette was rinsed with nanopure water three times prior to each new sample. Samples were analyzed from 800 to 200 nm at 1 nm increments. Three to four replicates per sample were scanned. "Blank" samples of nanopure water were scanned periodically throughout sample analyses as well as prior to and following scans of all analyzed samples.

Following collection of the spectrophotometer file, spectral data were copied into a spreadsheet of absorption values from 200 to 800 nm. Samples were blank-corrected by subtracting the average blank absorbance at each wavelength from sample absorbance at the same wavelength. Backscatter adjustments were made by subtracting the average absorbance for the same sample across wavelengths 700 to 800 nm from each wavelength's blank corrected sample absorbance (as recommended by Green and Blough, 1994). Diluted samples were adjusted to original absorbance values by multiplying the blank-and-backscatter-corrected absorbance by the total volume of the diluted sample over the original volume of undiluted sample.

a. Absorption Coefficient

Absorption coefficients were calculated using the equation;

$$Absorption\ Coefficient = \frac{2.303 * (corrected\ absorbance)}{path\ length\ of\ cuvette}$$

where the corrected absorbance is the absorbance value corrected for blank, backscatter, and dilution adjustments. The path length of the cuvette for all samples was 0.010m. The absorption coefficient was then used to calculate e2/e3 and $SUVA_{254}$ (see below) for each sample.

b. E2/E3

The ratio of absorption coefficients at 250 nm and 365 nm was calculated as the e2/e3 value for each sample and the standard deviation was less than 4.5% for each sample. In this ratio, 250 nm (e2) is representative of smaller molecular size, aromatic ring structures and 365 nm (e3) is representative of the larger molecular size, more aliphatic, long chain carbon groups. Smaller molecules have less absorption at longer wavelengths. Thus, an increase in the ratio of e2/e3 indicates a decrease in molecular size and aromaticity (Peuravuori and Pihlaja, 1997; Uyguner and Bekbolet, 2005).

c. Specific Ultraviolet Absorption, $SUVA_{254}$

The $SUVA_{254}$ value provides a DOC-concentration-normalized value for the specific UV absorption coefficient at 254 nm. $SUVA_{254}$ was calculated using the equation;

$$SUVA_{254} = \frac{Absorption\ coefficient\ at\ 254nm}{organic\ carbon\ concentration}$$

where the total organic carbon concentration is given in units of mg/L. The standard deviation was less than 4% for each sample. Increases in $SUVA_{254}$ correlate to increases in aromaticity of the sample (Weishaar et al., 2003).

2.7 Irradiation Monitoring

To analyze photodegradation, samples were exposed to natural sunlight for six hours (Figure 7). June samples from Amity Creek and the French River were monitored for exposure to irradiation using an Eppley Radiometer (model 8-1.8). Compared with reference standards, the Eppley derived value of the constant for this radiometer was $11.23 \bullet 10^{-6}$ V/Wm^{-2}. All other samples were monitored for irradiation using a Campbell Scientific LI200X-L pyranometer (model 97009). The pyranometer was calibrated against an Eppley pyranometer (precision spectral; PSP). Specifications include ±5% maximum (±3% typical) absolute error in natural daylight and a sensitivity of 0.2 kW m^{-2} mV^{-1}. The radiometers measured between wavelengths of 400 nm (violet) to 1100 nm (near infrared).

Figure 7. Photo-irradiation setup for photodegradation treatment with temperature sensor shown at the far left, "Exp" quartz flasks submerged in water bath at center, and irradiation sensor shown in lower right.

2.8 Microbial Enumeration

Epifluorescence microscopy was conducted on preserved samples stained with 200μg/mL 4'6' –Diamidine-2'-phenylindole dihydrochloride (DAPI, Roche Diagnostics) and filtered onto 0.2μm black polycarbonate membrane filters (Millipore 0.22μm GTBP). Samples were preserved by taking 9mL sample and mixing with 1mL 20% certified ACS formaldehyde (Fisher Scientific). The preserved samples were stored in the dark at 4°C for up to four days prior to staining and slide preparation. Slide preparation was performed with all lights in the laboratory turned off.

A side arm flask was set up with a 25mm uncombusted GFF filter (Whatman). Using a hand vacuum pump, 3ml Milli-Q water was filtered as a rinse. A black polycarbonate filter was placed on top of the GFF and vacuum pressure was removed. 100μL of 200μg/mL DAPI was added to the 10mL of preserved sample (9mL:1mL sample: formaldehyde) and poured into the filtration setup, covered with foil to block any light penetration, and left for five minutes (Figure 8). After five minutes, vacuum pressure (≤0.03 MPa) was applied using the hand pump to filter out all liquid. The black filter was then placed on a slide (Corning) with a drop of immersion oil (Cargille, type FF) and a microscope cover glass (No. 1 thickness, Esco; Figure 9). Excess oil was blotted off and the slide was labeled and stored in a dark box in the laboratory freezer.

Microbial enumerations were conducted using a Nikon Eclipse TS100 epifluorescence microscope at the University of Minnesota Duluth. Fluorescence was initiated with an EXFO X-Cite (series 120 Q) 120 W mercury vapor short arc lamp on

slides stained with 200µg/mL DAPI. Bacterial enumerations were conducted using the equation;

$$\frac{(filteredarea \bullet \#microbes)}{(mL\ filtered \bullet count\ area)} \equiv microbes/mL$$

where the filtered area was equal to 200,960,000µm^2.

Figure 8. Epi-fluorescence microscopy slide preparation setup.

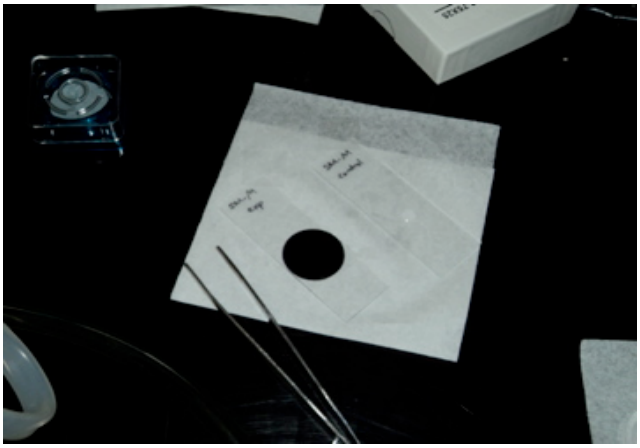

Figure 9. 4'6' –Diamidine-2'-phenylindole dihydrochloride stained black filter of formaldehyde-preserved sample.

2.9 Microbial Degradation

Replicate volumes of the base flow June 2010 “init” samples were collected to study the microbial degradation of DOM. “Init” samples were divided into six replicate 40mL samples for each “init” sample and placed in 50mL Erlenmeyer flasks with stoppers. Three of the replicate samples, “innoc” (samples 1, 2, and 3) were inoculated with 1mL of unfiltered Lake Superior water (“LS WHOLE” in Tables 16 and 17). The remaining replicate samples, “control” (samples 4, 5, and 6) were not inoculated with Lake Superior microbes.

The unfiltered Lake Superior water used for inoculations was collected in an acid rinsed carboy on the Western shore of Lake Superior less than one mile from the laboratory. The carboy was rinsed with sample water three times prior to final sample collection. The sample was then transported to the laboratory, and “init” samples 1, 2, and 3 were inoculated within one hour of Lake Superior water collection. “Start” samples were collected for TOC, UV-Vis, and epi-fluorescence microscopy analyses.

After adding inoculant to samples 1-3, all samples (1-6) from each river were stored with stoppers in place, inside a box covered with foil to block out sunlight. The room temperature was 69.0°F, stabilized by air conditioning. Once every 24 hours, each flask was uncapped and swirled to prevent sample anoxia. Air conditioning was turned off during mixing to prevent sample contamination by air dust particles. After 96 hours of inoculation, “end” samples were collected for TOC, UV-Vis, and epi-fluorescence microscopy analyses.

3. Results and Discussion

3.1. Photodegradation experiments

Results for $SUVA_{254}$, e2/e3, and organic carbon concentration are shown in Tables 4, 5, and 6 respectively.

3.1.a. Specific UV-absorption at 254nm

Table 4. Measured $SUVA_{254}$ values (mg $C \bullet L^{-1} \bullet m^{-1}$) for all samples.

	Whole	Init	Start	Exp	Control
SM1-Gb	13.67	10.80	11.06	10.53	10.90
SM1-F	6.92	6.42	8.78	8.74	9.33
SM1-Am	8.16	10.41	8.53	7.83	8.51
SM1-K	7.62	5.98	9.11	8.79	9.27
SM1-M	3.42	2.48	2.27	2.17	2.28
SM2-Gb	13.67	10.80	9.87	9.66	9.83
SM2-F	6.92	6.42	7.83	7.27	7.59
SM2-Am	8.16	10.41	7.23	7.28	7.51
SM2-K	7.62	5.98	7.82	7.39	7.88
SM2-M	3.42	2.48	2.58	2.44	2.57

	Whole	Init	Start	Exp	Control
GB-June	8.97	7.50	9.09	9.04	9.17
F-June	9.14	6.19	9.40	9.51	9.92
Am-June	6.88	6.06	8.23	7.74	8.08
K-June	9.63	9.13	14.70	13.89	14.12
M-June	8.71	7.38	8.71	9.12	9.40
GB July	8.98	8.49	9.27	9.16	9.41
F Aug	9.79	9.07	9.91	9.32	9.58
Am Aug	8.67	7.98	9.42	8.15	8.49
K Aug	13.73	12.61	12.92	13.70	13.33
M Aug	9.44	8.31	9.56	8.99	9.47

The values in Tables 4 show the variance in each of the different river sites. The $SUVA_{254}$ values shown in Table 4 reflect that the most urban sample site, Miller Creek, has the lowest $SUVA_{254}$ value of 3.42 mg $C \bullet L^{-1} \bullet m^{-1}$ for the "whole" sample during the snow melt season. Likewise, the most rural sample site, Gooseberry River, has the

highest $SUVA_{254}$ value of 13.67 mg $C \bullet L^{-1} \bullet m^{-1}$ for the "whole" sample during the snow melt season. The increased $SUVA_{254}$ value shows that the rural sample site at the Gooseberry River has more aromatic DOM than the more urban Miller Creek sample site during the snow melt season. Base flow samples do not show a trend in $SUVA_{254}$.

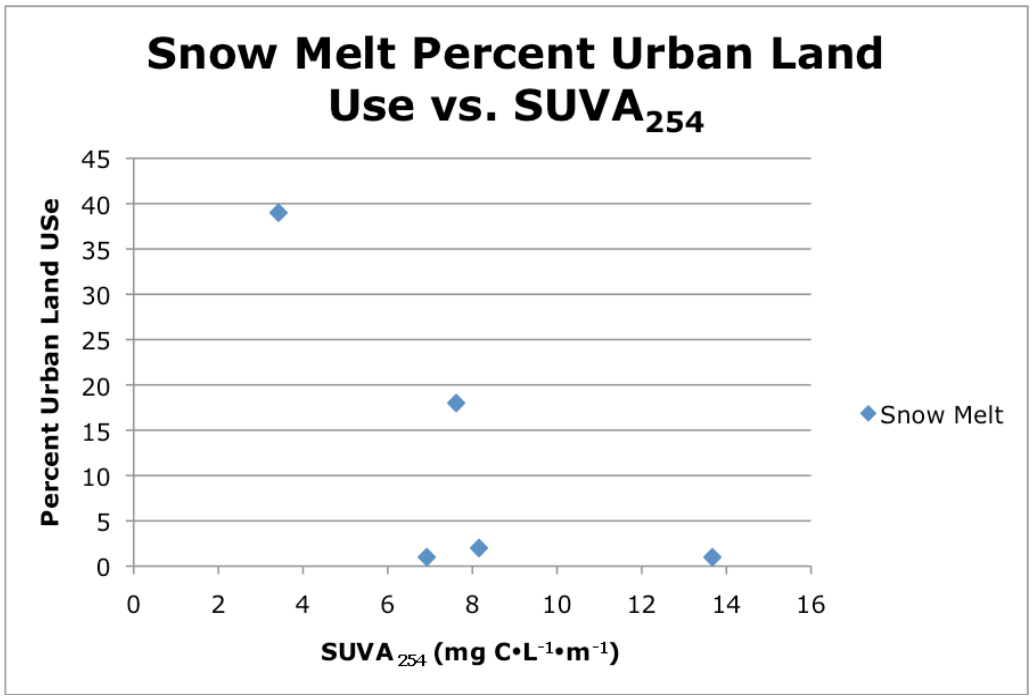

Figure 10. Percent urban land use in watershed vs. $SUVA_{254}$ for "whole" snow melt samples. Error bars are smaller than the data marker for all data points.

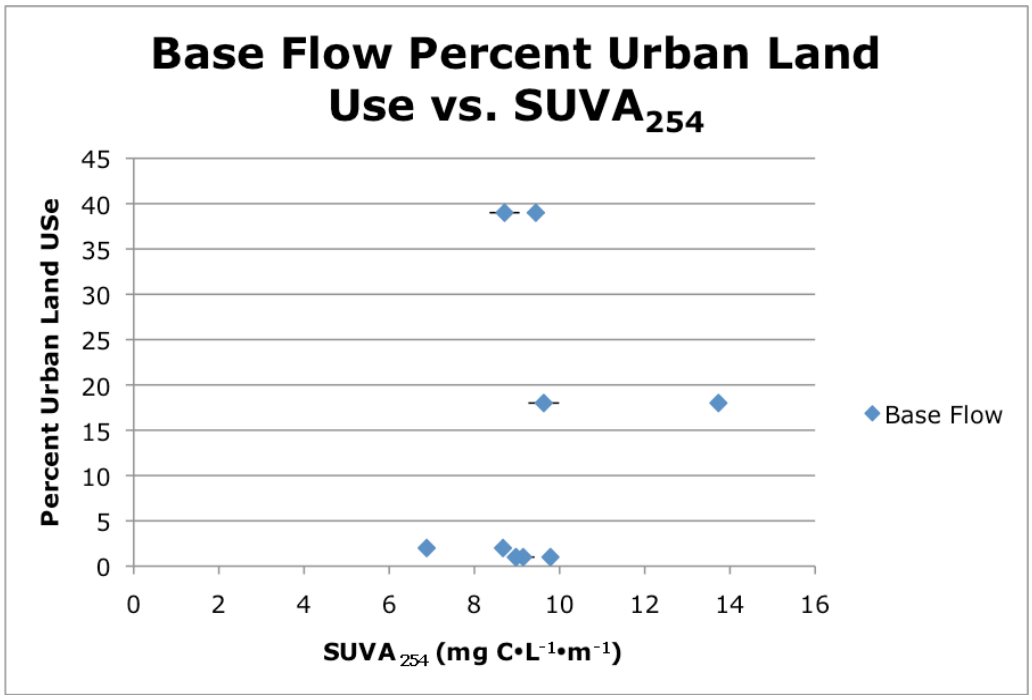

Figure 11. Percent urban land use in watershed vs. $SUVA_{254}$ for "whole" base flow samples. Error bars are the propogated error from UV-Vis and DOC analytical precision.

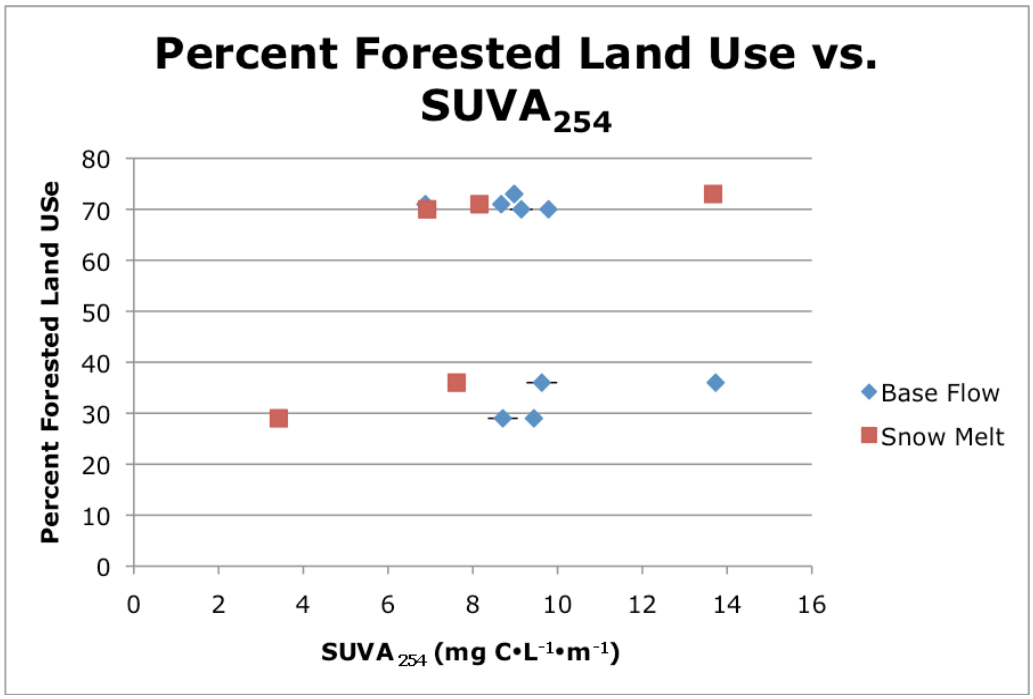

Figure 12. Percent forested land use in watershed vs. $SUVA_{254}$ for all "whole" samples. Error bars are the propogated error from UV-Vis and DOC analytical precision

3.1.b. E2/E3

Table 5. Measured e2/e3 values for all samples.

	Whole	Init	Start	Exp	Control
SM1-Gb	4.29	5.21	5.16	5.54	5.18
SM1-F	4.89	5.52	5.34	5.8	5.35
SM1-Am	4.96	4.64	5.8	6.33	5.86
SM1-K	3.98	5.59	5.37	5.84	5.34
SM1-M	4.21	6.11	5.76	6.4	5.77
SM2-Gb	4.29	5.21	5.12	5.52	5.12
SM2-F	4.89	5.52	5.3	5.79	5.4
SM2-AM	4.96	4.64	5.79	6.33	5.76
SM2-K	3.98	5.59	5.28	5.78	5.26
SM2-M	4.21	6.11	5.77	6.25	5.65

	Whole	Init	Start	Exp	Control
GB June	4.75	5.21	5.23	5.51	5.15
F June	5.02	5.3	5.11	5.44	5.05
Am June	5.22	5.52	5.09	5.92	5.24
K June	4.82	5.11	4.49	4.91	4.58
M June	5.5	5.9	5.2	5.46	4.91
GB July	5.28	6.14	5.93	6.32	5.86
F Aug	5.31	5.52	5.3	6.08	5.52
Am Aug	5.69	5.87	4.97	6.52	6.03
K Aug	4.37	4.58	4.59	4.84	4.58
M Aug	5.36	6.14	5.48	6.2	5.69

Table 5 shows e2/e3 values for the whole water and initial filtered samples and the photodegradation experiment. Whole samples show very little variation across sample sites, indicating that the molecular size of the constituents of DOM at each site is similar. However, seasonal variations across sample sites are shown. The base flow season "whole" samples all have a higher e2/e3 value than the snow melt "whole" samples. Base flow "whole" samples had a significantly higher e2/e3 ratio (average of 5.13, range 4.37 to 5.69) than snow melt "whole" samples (average of 4.47, range 3.98 to 4.96)

(p=0.0008, two sample t-test assuming equal variance, t=3.70). “Init” samples do not show statistically significant seasonal sample variation (p=0.3, two sample t-test assuming equal variance, t=0.511).This signifies the presence of OM constituents that are smaller in molecular size for the unfiltered base flow samples, and OM constituents that are larger in molecular size for the snow melt samples.

3.1.c. Organic Carbon Concentrations

Table 6. Organic carbon concentrations (mg/L) for all samples. Uncertainties are the standard deviations from replicate (n=3 to 5) injections of the sample.

	Whole	Init	Start	Exp	Control
SM1-Gb	13.36	13.48	11.41 ± 0.37	11.36 ± 0.08	11.27 ± 0.09
SM1-F	6.15	5.81	4.62 ± 0.05	4.47 ± 0.01	4.41 ± 0.02
SM1-Am	6.89	6.64	5.7 ± 0.19	5.85 ± 0.01	5.7 ± 0.004
SM1-K	6.1	7.61	5.49 ± 0.11	5.41 ± 0.005	5.42 ± 0.02
SM1-M	16.6	17.78	19.02 ± 0.37	18.95 ± 0.12	18.97 ± 0.06
SM2-Gb	13.36	13.48	12.28 ± 0.02	12.06 ± 0.13	12.32 ± 0.08
SM2-F	6.15	5.81	5.26 ± 0.07	5.39 ± 0.03	5.39 ± 0.14
SM2-AM	6.89	6.64	6.62 ± 0.06	6.45 ± 0.08	6.57 ± 0.09
SM2-K	6.1	7.61	6.51 ± 0.05	6.53 ± 0.03	6.41 ± 0.01
SM2-M	16.6	17.78	17.17 ± 0.13	17.28 ± 0.02	17.11 ± 0.09

	Whole	Init	Start	Exp	Control
GB June	26.01	26.18	22.39 ± 0.40	22.03 ± 0.26	22.43 ± 0.02
F June	16.08	23.15	15.56 ± 0.06	15.15 ± 0.00	15.26 ± 0.01
Am June	14.57	17.11	12.95 ± 0.16	12.26 ± 0.38	12.78 ± 0.12
K June	15.5	15.8	11.06 ± 0.39	10.77 ± 0.05	10.88 ± 0.10
M June	12.01	13.68	11.75 ± 0.16	11.22 ± 0.001	11.58 ± 0.014
GB July	10.81	10.39	9.66 ± 0.12	9.52 ± 0.008	9.58 ± 0.04
F Aug	15.16	16.2	15.25 ± 0.18	15.1 ± 0.01	15.17 ± 0.05
Am Aug	10.23	10.73	10.37 ± 0.18	10.16 ± 0.003	10.17 ± 0.002
K Aug	27.62	29.44	27.26 ± 0.42	26.19 ± 0.05	27.46 ± 0.19
M Aug	12.34	13.2	11.83 ± 0.19	11.91 ± 0.002	11.84 ± 0.007

Organic carbon concentrations and error analyses based on replicate injections are shown in Table 6. The difference between “whole” and “init” sample concentrations may be due to sorption of OC to particles, and settling during the testing sequence (Minor et al., unpublished). The settling of OC with large particles may explain why in some cases, the OC concentration is higher for the “init” sample than the “whole” sample, since there are more large particles available in the “whole” to effectively remove OC from the sample volume analyzed by the instrument.

The Miller Creek snow melt 1 (SM1) sample increase in OC concentration from the “init” to the “start” sample may be due to contamination during refrigerator storage or to coagulation/precipitation of organic matter into colloids and particles coupled with incomplete sample mixing prior to injection (Chin et al, 1998). Decreases from “init” to “start” in the remaining samples may result from respiration of organic carbon to inorganic carbon dioxide by a minimal population of microbes present in the samples.

3.2. Normalized Results

Normalization of experimental samples was performed to allow for comparisons among samples as a function of experimental manipulation. For normalized samples, "Exp" and "Control" data show the difference between the "Start" sample and the "Exp" or "Control" samples using the equation;

$$Normalized\ value = test\ sample - "Start"$$

Where "test sample" indicates "Exp" or "Control". Normalized results for $SUVA_{254}$, e2/e3, and organic carbon concentration are shown in tables 7, 10, and 12 respectively. Negative values indicate samples that showed a decrease in $SUVA_{254}$, e2/e3, or organic carbon concentration from the "start" sample to the test sample.

For better insight into the degree of alteration a sample exhibited upon manipulation, percent change for experimental and control samples were calculated using the equation;

$$Percent\ Change = \frac{(test\ sample - "start")}{"start"} * 100$$

where "test sample" indicates "Exp" or "Control". Propagation of uncertainty from random error for percent change results was calculated using absolute uncertainty for mixed operations (Harris, 2007).

3.2.a. Specific UV-Absorption at 254nm

Table 7. Normalized $SUVA_{254}$ values (mg $C \bullet L^{-1} \bullet m^{-1}$) for all samples.

	Exp	Control	Exp St.Dev	Cont. St.Dev
SM1-Gb	-0.54	-0.16	0.01	0.07
SM1-F	-0.04	0.55	0.08	0.01
SM1-Am	-0.70	-0.02	0.12	0.03
SM1-K	-0.32	0.16	0.01	0.02
SM1-M	-0.10	0.01	0.01	0.01
SM2-Gb	-0.21	-0.04	0.03	0.02
SM2-F	-0.56	-0.24	0.02	0.01
SM2-Am	0.05	0.28	0.05	0.02
SM2-K	-0.42	0.07	0.00	0.03
SM2-M	-0.13	-0.01	0.01	0.05

	Exp	Control	Exp St.Dev	Cont. St.Dev
GB-June	-0.05	0.08	0.10	0.07
F-June	0.11	0.52	0.03	0.06
Am-June	-0.49	-0.15	0.05	0.09
K-June	-0.81	-0.57	0.09	0.04
M-June	0.41	0.69	0.05	0.09
GB July	-0.11	0.15	0.03	0.06
F Aug	-0.59	-0.32	0.04	0.04
Am Aug	-1.28	-0.93	0.02	0.01
K Aug	0.78	0.42	0.02	0.04
M Aug	-0.57	-0.09	0.01	0.01

Table 8. Percent change in $SUVA_{254}$ results.

	Exp Percent Change	Control Percent Change	Exp Absolute Uncertainty	Control Absolute Uncertainty
SM1-Gb	-4.860	-1.475	0.02	0.02
SM1-F	-0.463	6.299	0.009	0.002
SM1-Am	-8.240	-0.243	0.04	0.03
SM1-K	-3.492	1.732	0.002	0.002
SM1-M	-4.402	0.648	0.004	0.004
SM2-Gb	-2.157	-0.412	0.004	0.003
SM2-F	-7.180	-3.093	0.006	0.004
SM2-Am	0.672	3.829	0.007	0.004
SM2-K	-5.415	0.861	0.003	0.006
SM2-M	-5.205	-0.338	0.009	0.02

	Exp Percent Change	Control Percent Change	Exp Absolute Uncertainty	Control Absolute Uncertainty
GB-June	-0.500	0.876	0.01	0.007
F-June	1.164	5.545	0.02	0.03
Am-June	-6.004	-1.803	0.03	0.04
K-June	-5.498	-3.906	0.007	0.002
M-June	4.704	7.879	0.008	0.01
GB July	-1.164	1.570	0.004	0.007
F Aug	-5.955	-3.251	0.005	0.005
Am Aug	-13.536	-9.877	0.002	0.001
K Aug	6.068	3.224	0.002	0.003
M Aug	-5.972	-0.929	0.001	0.001

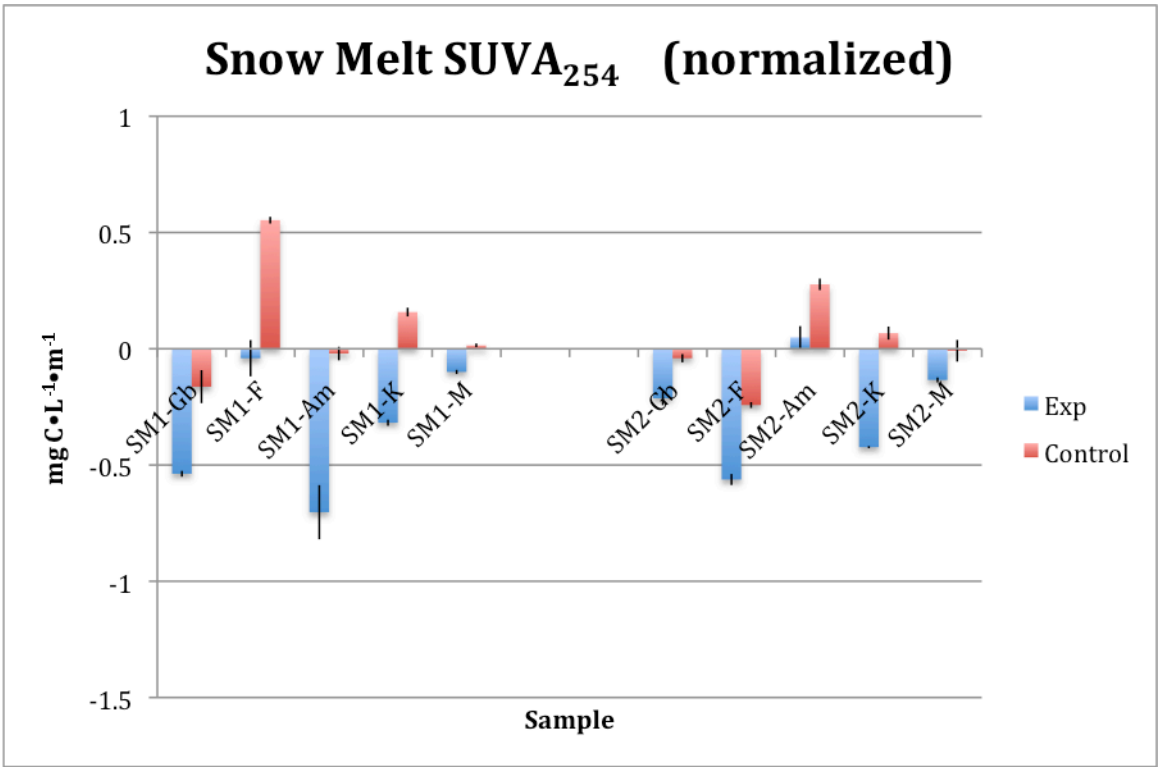

Figure 13. Normalized $SUVA_{254}$ (test sample – "start") results for snow melt samples.

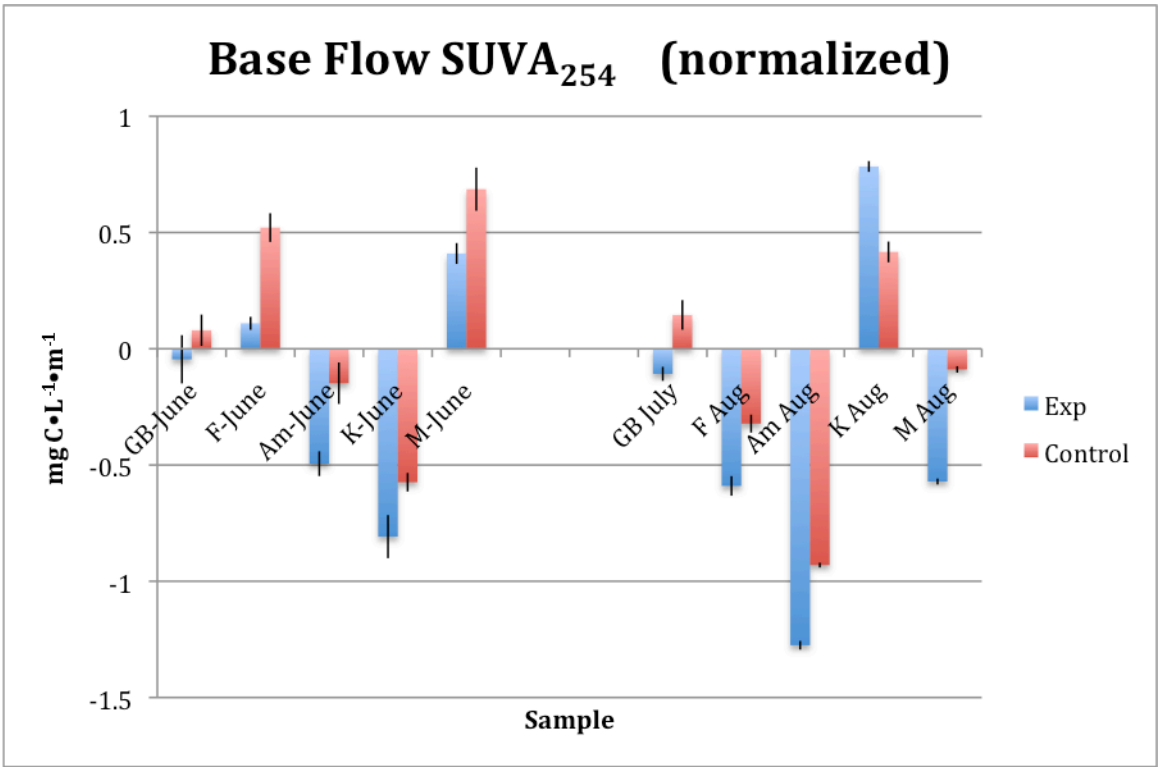

Figure 14. Normalized $SUVA_{254}$ (test sample – "start") results for base flow samples.

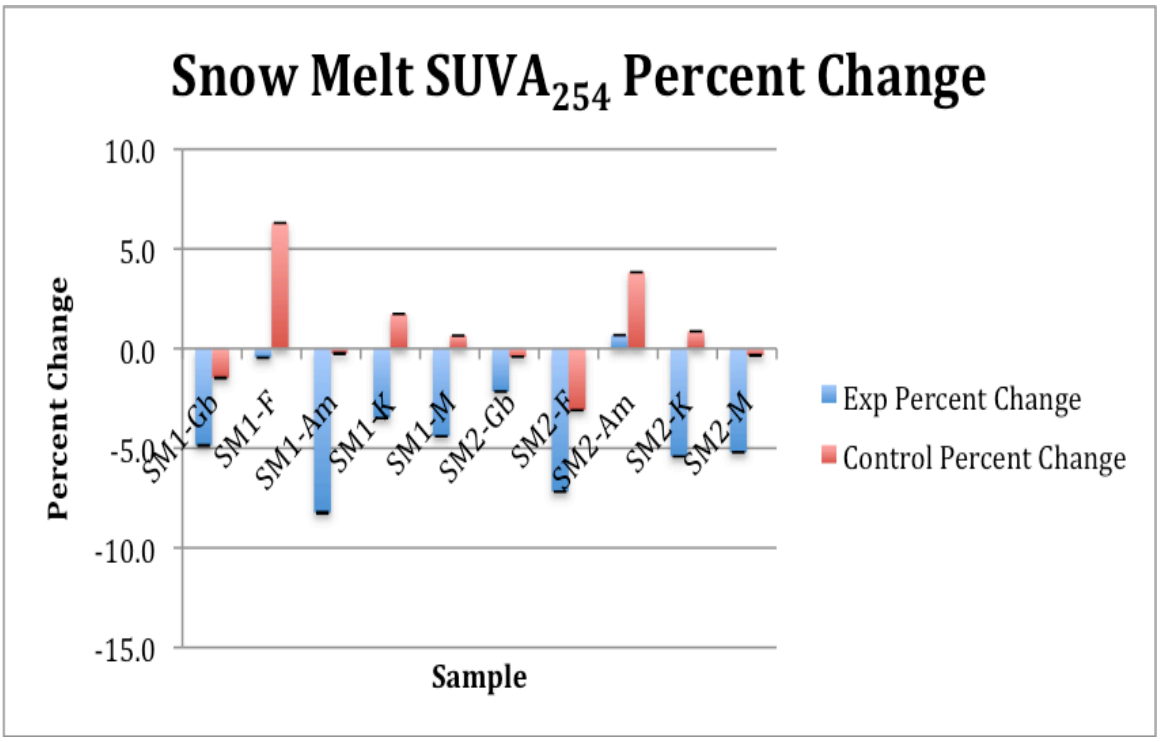

Figure 15. Percent change in snow melt sample $SUVA_{254}$. Error bars show the absolute standard deviation.

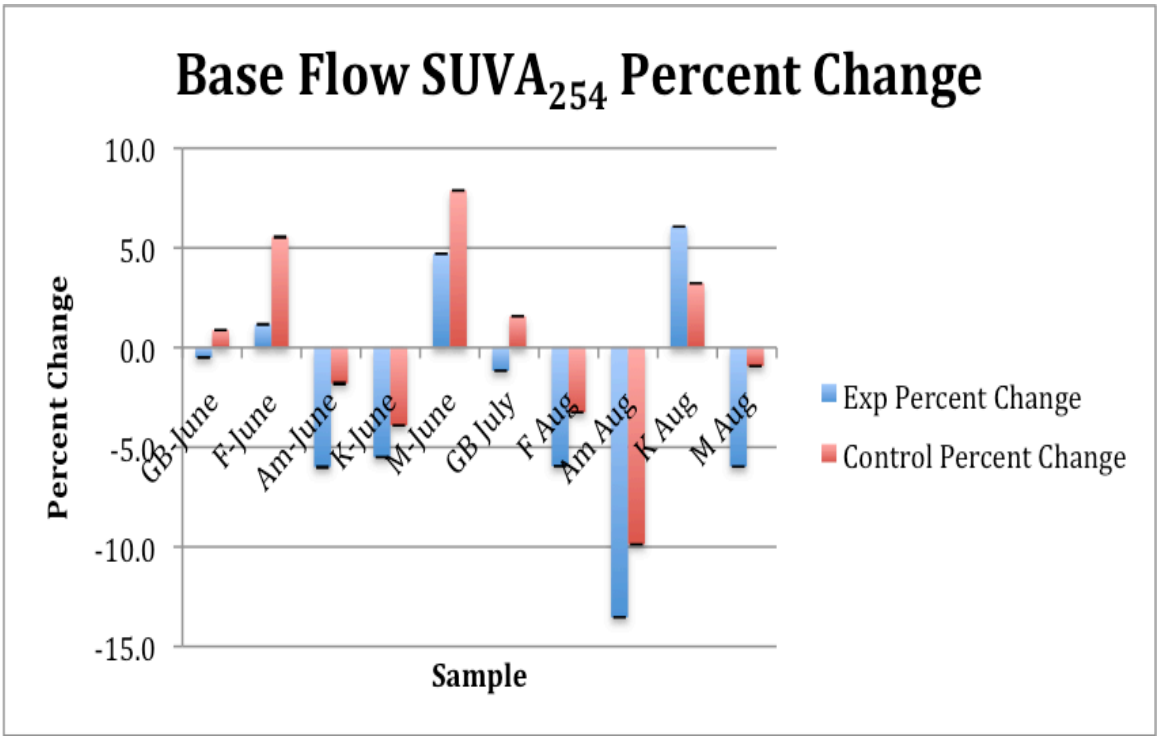

Figure 16. Percent change in base flow sample $SUVA_{254}$. Error bars show the absolute standard deviation.

Table 9. Comparison of percent change due to irradiation of snow melt versus base flow samples using a two sample t-test assuming equal variances; α=0.05, variable 1= snow melt samples, variable 2= base flow samples.

Sample Site	t Stat	P(T<=t) one tail
Gb	1.923	0.097
F	0.291	0.399
Am	-1.026	0.206
K	0.808	0.252
M	0.779	0.259

Table 7 and Figures 13 and 14 show the normalized $SUVA_{254}$ results. All snow melt samples except Amity Creek SM2 show a decrease in $SUVA_{254}$ upon photodegradation. All base flow samples except the June Miller Creek, June French River, and August Kingsbury Creek samples also show experimental samples with a loss in $SUVA_{254}$. Urbanization of sample sites may play a role in these observed trends. Kingsbury Creek and Miller Creek, the two most urban sample sites, show a higher $SUVA_{254}$ in the filtered "init" sample for base flow season. Amity Creek, the French River, and the Gooseberry River all have higher "init" $SUVA_{254}$ values for the snow melt sample season (Table 4) and this aromatic material appears to be photoreactive. None of the sample sites show significant statistical variation in the percent change in $SUVA_{254}$ as a function of season (Table 9).

The loss of specific UV-absorption upon irradiation corresponds to a loss of aromaticity in the photodegraded experimental samples. DOM molecules containing aromatic carbon are known to absorb UV light (Weishaar et al., 2003; Moran et al., 2000; Cory et al., 2007). As a result of photodegradation, the aromatic components of DOM in nine of the ten snowmelt samples and in seven of the ten base flow samples break down and the aromaticity of the DOM is reduced.

3.2.b. E2/E3

Table 10. Normalized e2/e3 values for all samples. Standard deviations are given for replicate analyses (n=3) of test samples from the same vial.

	Exp	Control	Exp Standard Deviation	Control Standard Deviation
SM1-Gb	0.38	0.02	0.04	0.02
SM1-F	0.46	0.01	0.08	0.03
SM1-Am	0.53	0.06	0.05	0.04
SM1-K	0.47	-0.03	0.09	0.02
SM1-M	0.64	0.01	0.03	0.00
SM2-Gb	0.40	0.00	0.01	0.03
SM2-F	0.49	0.10	0.07	0.03
SM2-Am	0.54	-0.03	0.03	0.07
SM2-K	0.50	-0.02	0.01	0.10
SM2-M	0.48	-0.12	0.04	0.06
	Exp	**Control**	**Exp Standard Deviation**	**Control Standard Deviation**
GB-June	0.28	-0.08	0.02	0.02
F-June	0.33	-0.06	0.04	0.04
Am-June	0.83	0.15	0.01	0.02
K-June	0.42	0.09	0.07	0.02
M-June	0.26	-0.29	0.05	0.06
GB July	0.39	-0.07	0.08	0.04
F Aug	0.78	0.22	0.12	0.03
Am Aug	1.55	1.06	0.06	0.02
K Aug	0.25	-0.01	0.01	0.01
M Aug	0.72	0.21	0.02	0.02

Table 11. Percent change in e2/e3 results.

	Exp Percent Change	Control Percent Change	Exp Absolute Uncertainty	Control Absolute Uncertainty
SM1-Gb	7.364	0.388	0.009	0.006
SM1-F	8.614	0.187	0.02	0.008
SM1-Am	9.138	1.034	0.01	0.01
SM1-K	8.752	-0.559	0.02	0.008
SM1-M	11.111	0.174	0.01	0.008
SM2-Gb	7.812	0.000	0.007	0.003
SM2-F	9.245	1.887	0.01	0.009
SM2-Am	9.326	-0.518	0.008	0.01
SM2-K	9.470	-0.379	0.01	0.006
SM2-M	8.319	-2.080	0.01	0.02

	Exp Percent Change	Control Percent Change	Exp Absolute Uncertainty	Control Absolute Uncertainty
GB-June	5.354	-1.530	0.005	0.004
F-June	6.458	-1.174	0.009	0.02
Am-June	16.306	2.947	0.04	0.04
K-June	9.354	2.004	0.01	0.005
M-June	5.000	-5.577	0.02	0.02
GB July	6.577	-1.180	0.01	0.01
F Aug	14.717	4.151	0.02	0.009
Am Aug	31.187	21.328	0.01	0.007
K Aug	5.447	-0.218	0.004	0.002
M Aug	13.139	3.832	0.004	0.005

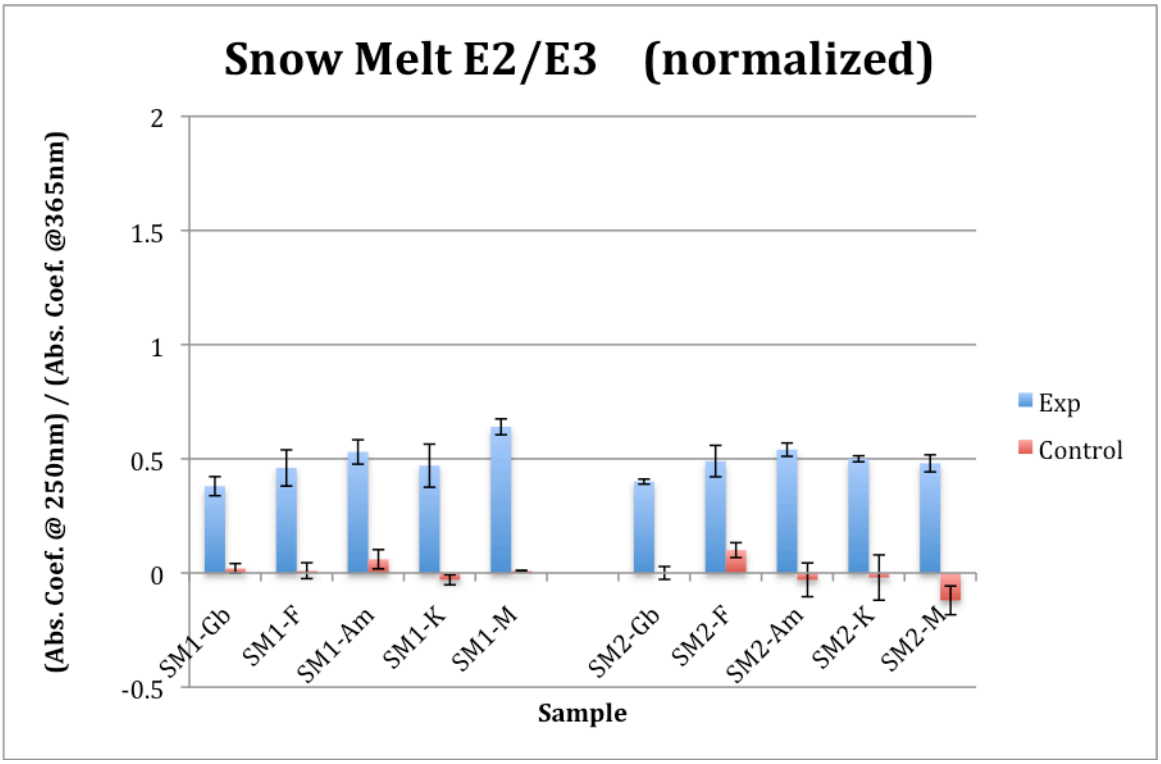

Figure 17. Normalized (test sample – "start") e2/e3 values for snow melt samples.

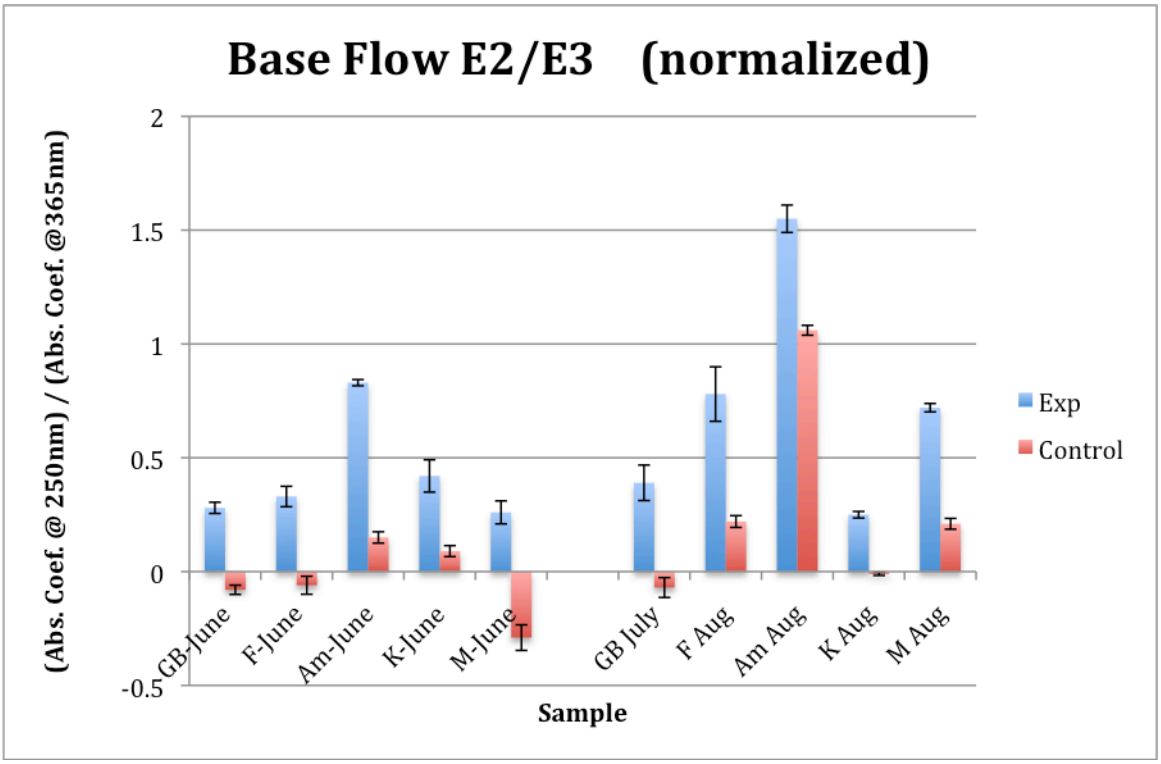

Figure 18. Normalized (test sample – "start") e2/e3 values for base flow samples.

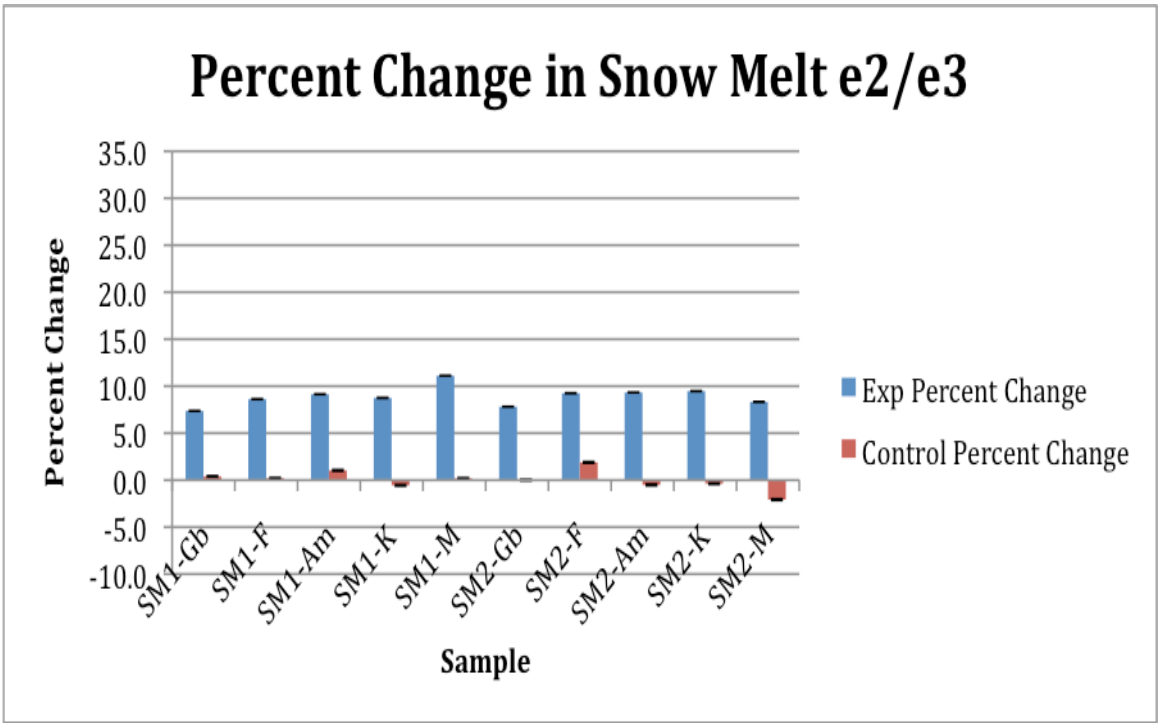

Figure 19. Percent change in e2/e3 for snow melt samples. Error bars show the absolute standard deviation.

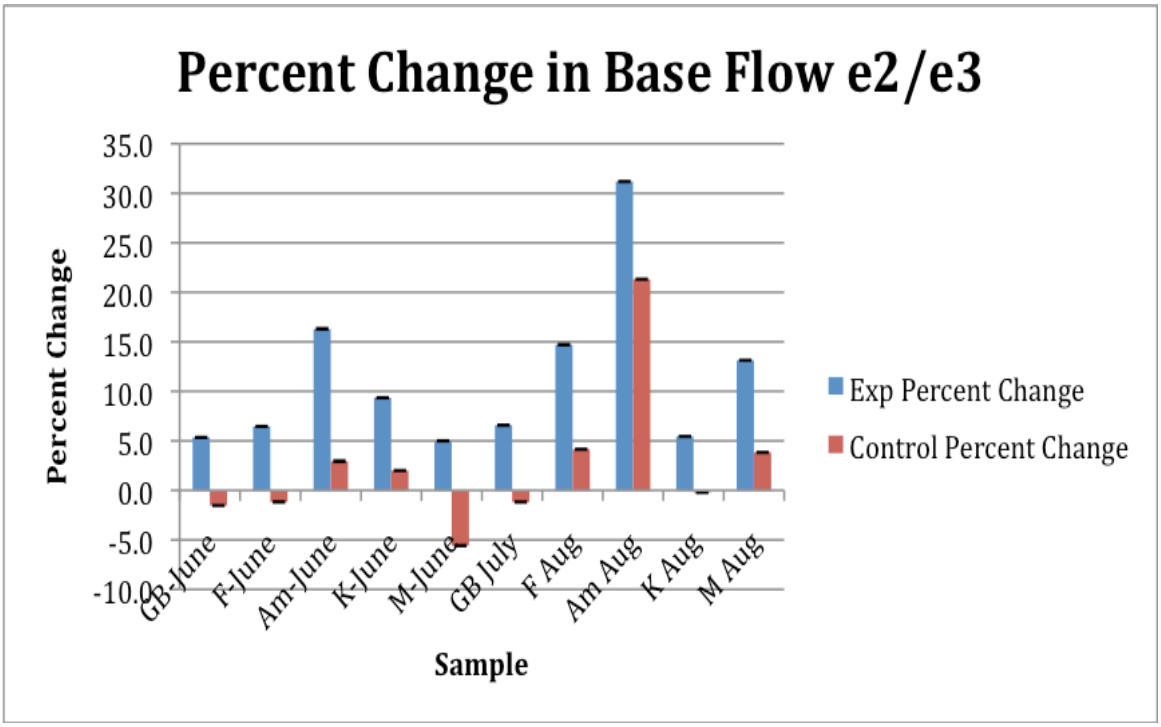

Figure 20. Percent change in e2/e3 for base flow samples. Error bars show the absolute standard deviation.

E2/e3 values are shown in Table 10 and Figures 17 and 18. All samples for base flow and snow melt show a greater increase in e2/e3 for the photodegraded experimental sample than for the control sample. The increase in e2/e3 following photodegradation corresponds to a decrease in molecular size. This is supported by the $SUVA_{254}$ data because a reduction in molecular size can often be accomplished through the removal of polymeric aromatic components of the DOM through bond cleavage.

Snow melt samples show a greater increase in e2/e3 upon photodegradation of experimental samples than base flow samples. This may be due to the increase in organic compounds (including pollutants) drained into a stream from the watershed due to high water flow through the upper soil column and overland during snow melt season (Meyer and Wania, 2008; Meyer et al., 2011; Wania, 1999; Macdonald et al., 2002): note that organic carbon concentration is often lower in snow melt than base flow (Table 6), as the inputs are diluted by the large amount of water also entering the stream. Preferential removal of the non-aromatic and/or larger components of DOM upstream of our sampling sites during base flow conditions, another possible explanation for difference in snow melt versus base flow e2/e3 response, does not seem likely based upon our measurements of "init" and "start" samples shown in Tables 4 & 5. In addition to increased input of organic matter during snow melt, the snow melt samples may have been subjected to less photodegradation prior to sample collection as a result of being blocked from sunlight exposure during snow cover. The release of organic matter during seasonal freeze-thaw cycles may also influence the e2/e3 values of snow melt samples (Feng et al., 2007) as shown in "whole" results (Table 5) but not in "start" samples. There

is not a discernable trend in e2/e3 values, or their shifts upon photodegradation, with relation to sample site land use.

3.2.c. Organic Carbon Concentrations

Table 12. Average normalized organic carbon concentrations (mg/L) for all samples, n=3 to 5 replicate injections.

	Exp	Control	Exp Standard Deviation	Control Standard Deviation
SM1-Gb	-0.05	-0.14	0.08	0.09
SM1-F	-0.15	-0.21	0.01	0.02
SM1-Am	0.15	0.00	0.01	0.00
SM1-K	-0.08	-0.07	0.01	0.02
SM1-M	-0.07	-0.05	0.12	0.06
SM2-Gb	-0.22	0.04	0.13	0.08
SM2-F	0.13	0.13	0.03	0.14
SM2-AM	-0.17	-0.05	0.08	0.09
SM2-K	0.02	-0.10	0.03	0.01
SM2-M	0.11	-0.06	0.02	0.09
	Exp	**Control**	**Exp Standard Deviation**	**Control Standard Deviation**
GB June	-0.36	0.04	0.26	0.02
F June	-0.41	-0.3	0.00	0.01
Am June	-0.69	-0.17	0.05	0.12
K June	-0.29	-0.18	0.03	0.36
M June	-0.53	-0.17	0.00	0.14
GB July	-0.14	-0.08	0.01	0.04
F Aug	-0.15	-0.08	0.01	0.05
Am Aug	-0.21	-0.20	0.00	0.00
K Aug	-1.07	0.20	0.05	0.19
M Aug	0.08	0.01	0.00	0.01

Table 13. Percent change in organic carbon concentration.

	Exp Percent Change	Control Percent Change	Exp Absolute Uncertainty	Control Absolute Uncertainty
SM1-Gb	-0.438	-1.227	0.08	0.2
SM1-F	-3.247	-4.545	-0.2	-0.08
SM1-Am	2.632	0.000	0.06	0.08
SM1-K	-1.457	-1.275	0.002	-0.03
SM1-M	-0.368	-0.263	0.05	0.1
SM2-Gb	-1.792	0.326	-2.2	-0.8
SM2-F	2.471	2.471	-0.008	-0.8
SM2-Am	-2.568	-0.755	0.1	0.1
SM2-K	0.307	-1.536	-0.08	-0.009
SM2-M	0.641	-0.349	0.2	0.1

	Exp Percent Change	Control Percent Change	Exp Absolute Uncertainty	Control Absolute Uncertainty
GB-June	-1.608	0.179	0.2	0.4
F-June	-2.635	-1.928	0.05	0.04
Am-June	-5.328	-1.313	-0.6	0.05
K-June	-2.622	-1.627	0.4	0.3
M-June	-4.511	-1.447	0.2	0.03
GB July	-1.449	-0.828	0.1	0.09
F Aug	-0.984	-0.525	0.2	0.1
Am Aug	-2.025	-1.929	0.2	0.2
K Aug	-3.925	0.734	0.4	0.3
M Aug	-0.676	0.085	0.2	0.2

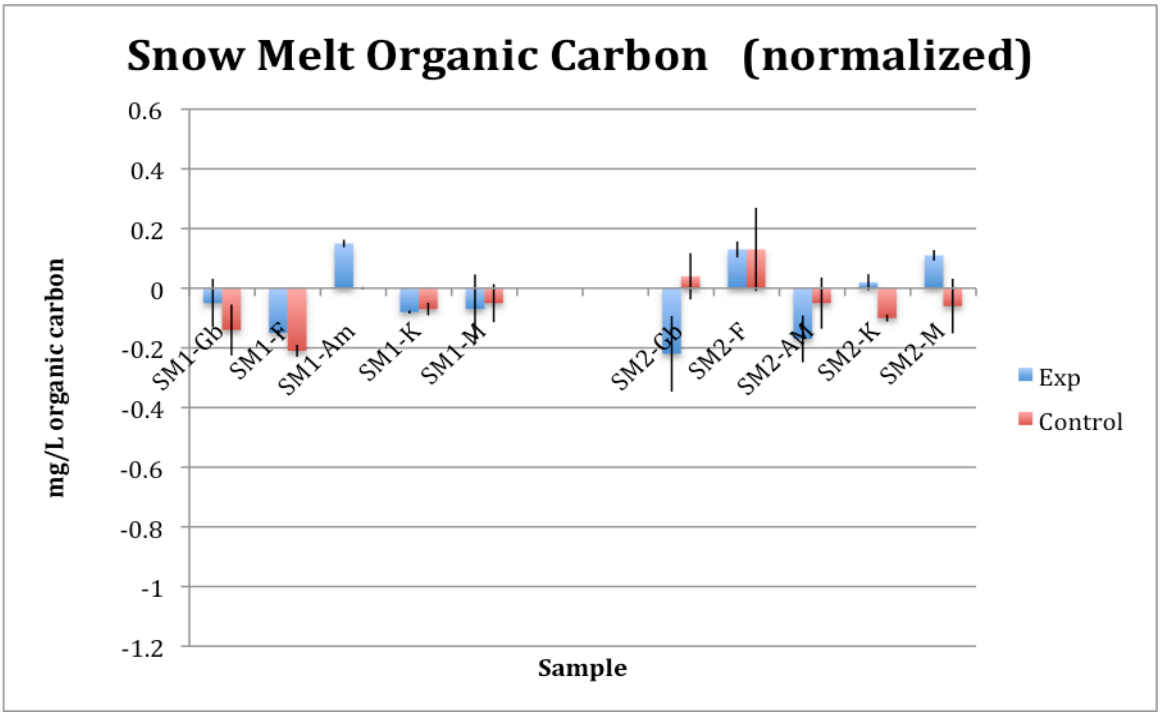

Figure 21. Normalized (test sample – "start") organic carbon concentrations for snow melt samples.

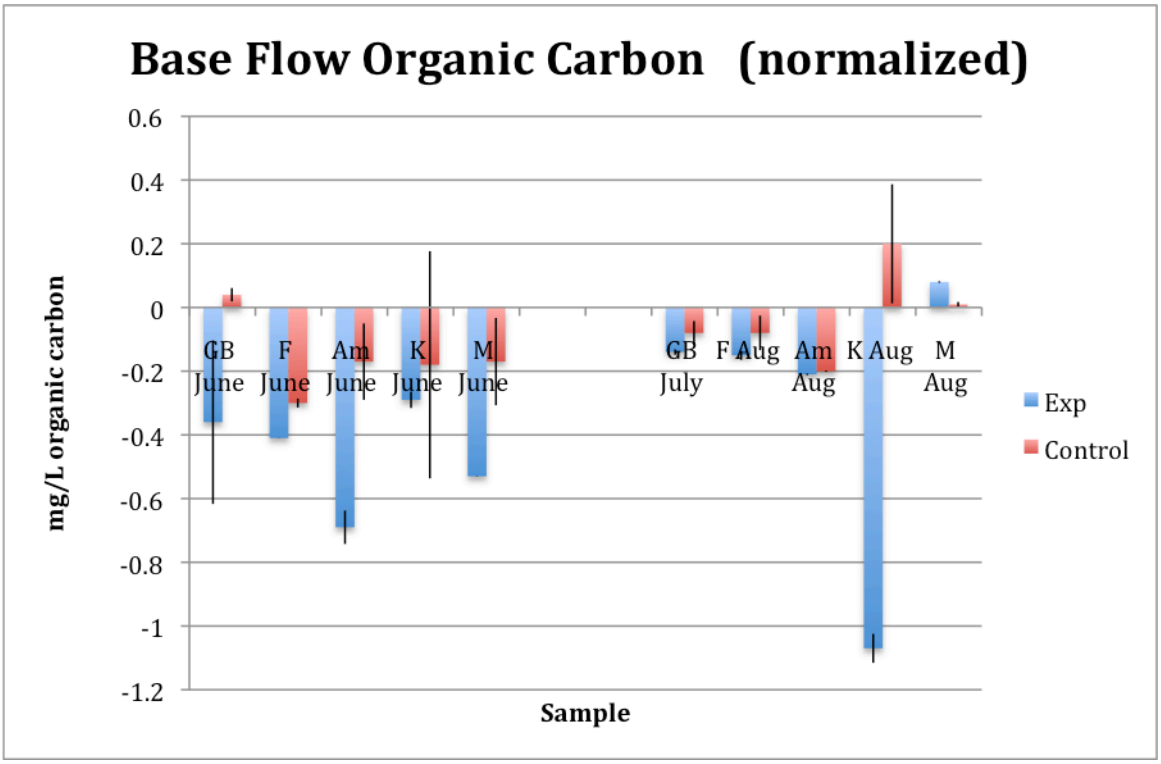

Figure 22. Normalized (test sample – "start") organic carbon concentrations for base flow samples.

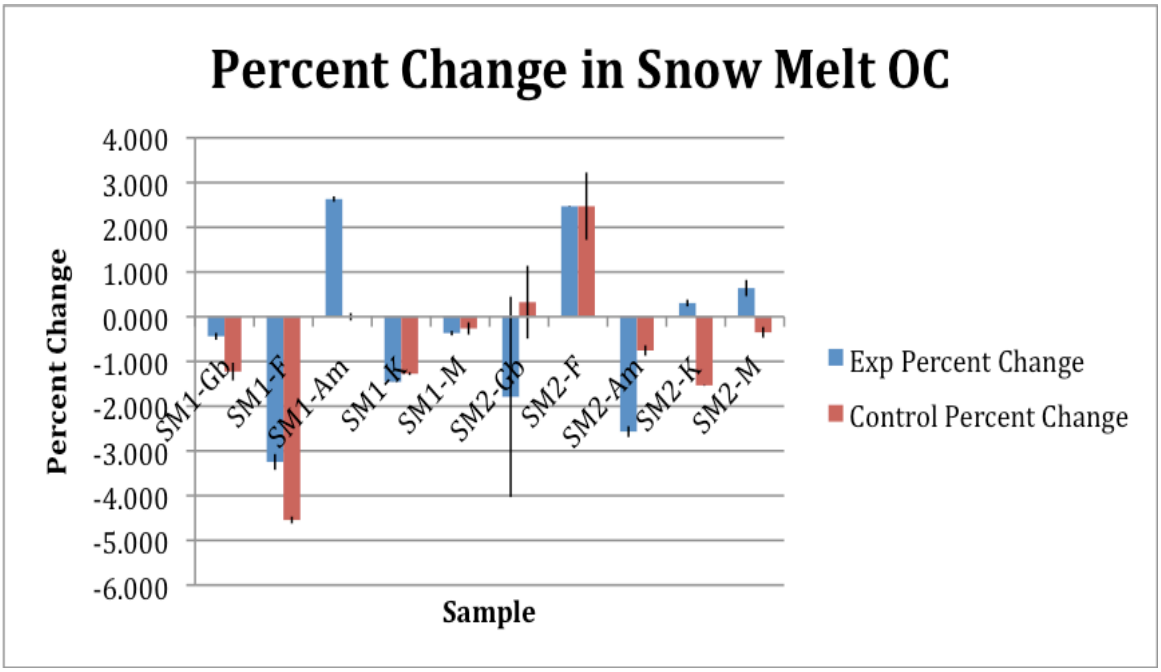

Figure 23. Percent change in snow melt organic carbon concentrations. Propagation of uncertainty as absolute standard deviation in replicate samples (n=3) is shown in error bars.

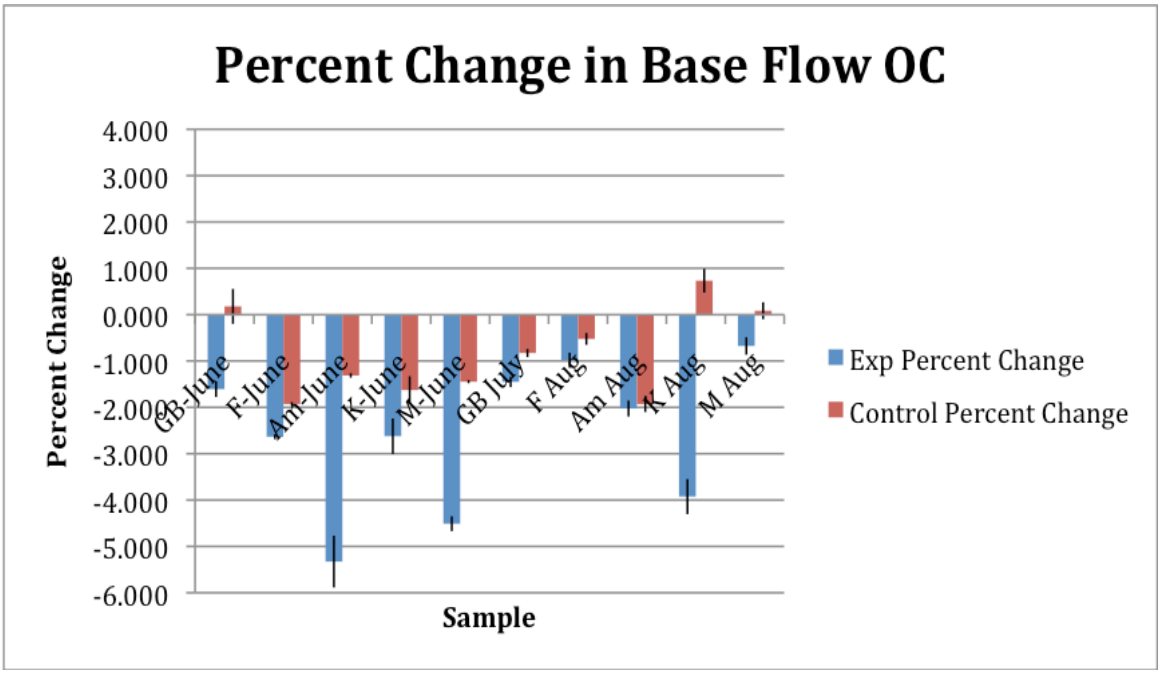

Figure 24. Percent change in base flow organic carbon concentrations. Propagation of uncertainty as absolute standarard deviation in replicate samples (n=3) is shown in error bars.

Normalized values of dissolved organic carbon are shown in Table 12, and Figures 21 and 22. Base flow samples show a loss of organic matter (measured as DOC) for nine of the ten samples following photodegradation treatments. Snow melt samples show varying responses in DOC concentration upon irradiation, with no measurable change in DOC concentration for most samples due to large sample standard deviations.

The most urban sample sites, Miller Creek (June) and Kingsbury Creek (August), showed the third-highest and highest reductions, respectively in DOC concentration (with the June Miller Creek sample and the August Kingsbury samples showing, respectively, the second and third greatest percent reduction in DOC) among the irradiated base flow samples. The $SUVA_{254}$ results showed that sixteen of the twenty samples had a loss in aromaticity upon irradiation of the DOM. The normalized e2/e3 results in Table 10 show that snow melt samples have the greatest reduction in molecular size as a result of photodegradation treatment.

Considering all of these factors with respect to photodegradation treatments: Table 12 shows that more DOC may be removed from the more urban sample sites, $SUVA_{254}$ results in Table 7 show a loss of aromaticity in the majority of treated samples, and normalized e2/e3 results indicate a greater reduction in molecular size for snow melt samples. Base flow DOM appears more likely to be remineralized (leading to losses in DOC) than snow melt DOM and urban stream DOM appears more susceptible to this remineralization. Snow melt DOM appears more likely to be altered in molecular size. The majority of samples across seasons show a loss of aromaticity upon irradiation.

3.3. Natural Solar Irradiance

Solar irradiance was measured throughout the photodegradation treatments. Multiple samples were irradiated on each photodegradation treatment day, as indicated in Table 14. Total irradiance was calculated as the sum of irradiance measured for the duration of sample exposure to natural solar irradiation, as shown;

$$Light\ Energy = \Delta t * \sum \frac{Watts}{m^2}$$

where the time interval between measurements was sixty seconds and the summation of W/m^2 was calculated for the time interval (multiplied by sixty seconds per minute) given in Table 14. All total irradiance values expressed in Table 14 have a mean value of 18.2± 1.38 MJ/m^2. Sample exposure times have a mean value of 360.17 ± 1.94 minutes.

Table 14. Irradiance measured during photodegradation treatment for all samples.

Date	Total Irradiance (MJ/m^2)	Irradiated Samples	Sample Exposure Time (minutes)
29-Jun-10	17.5	Am-June, F-June	362
9-Aug-10	17.9	Gb-June, Gb-July	360
22-Aug-10	20.1	Gb-Aug, M-June, K-June	361
29-Aug-10	16.8	Am-Aug, F-Aug, K-Aug, & M-Aug	362
28-Jun-11	17.1	SM1-(Am, F, Gb, K, & M)	357
13-Jul-11	19.7	SM2-(Am, F, Gb, K, & M)	359

3.4. Microbial enumeration in photodegradation experiment samples

Microbial enumerations were analyzed on samples from the June 2010 base flow sample season, as well as the snow melt samples (Table 15) in order to evaluate potential complications from microbial degradation within the photochemical experiments. Base flow samples from July and August 2010 were not analyzed via epi-fluorescence microscopy; however, these samples were stored for considerably less time prior to light exposure and should thus be less affected by microbial interactions than the June samples. The increase in microbial abundance during storage in the refrigerator shown by the difference between "init" and "start" samples in Table 15 suggests that bacterial growth occurred during the sample storage period prior to photodegradation and microbial degradation treatments. The microbial abundances of the "start" samples indicate that a portion of the photodegradation and microbial degradation treatments (even within the controls) may be due to the presence of a growing microbial population. As a result, microbial degradation treatments should be interpreted carefully, realizing that a truly abiotic control did not exist.

Table 15. Epifluorescence microscopy results in (microbes $\bullet 10^6$) per mL.

	Gb June	F June	Am June	K June	M June
Whole	1.3321	3.2449	3.0589	2.8058	2.2700
Init	0.0298	0.0372	0.0223	0.0223	0.0447
Start	0.7293	0.0223	0.3721	1.2429	0.9601
Exp	0.6995	0.2307	0.7294	1.3843	1.3844
Control	0.8782	0.3051	0.9675	1.6225	1.9277
	SM1-Gb	**SM1-F**	**SM1-Am**	**SM1-K**	**SM1-M**
Whole	2.2230	2.6944	2.4463	1.2157	1.2901
*Init**	0.0099	0.0099	0.0198	0.0397	0.0397
*Start**	0.2431	0.0744	0.1637	0.2531	0.0695
Exp	1.1214	0.9180	0.7691	0.9477	0.7493
Control	0.6897	0.3523	0.5111	0.5905	0.2382
	SM2-Gb	**SM2-F**	**SM2-Am**	**SM2-K**	**SM2-M**
Whole	2.2230	2.6944	2.4463	1.2157	1.2901
*Init**	0.0099	0.0099	0.0198	0.0397	0.0397
*Start**	0.1389	0.1389	0.2679	0.2134	0.2233
Exp	0.6996	1.4191	0.6252	1.9104	0.9577
Control	0.4019	0.3473	0.4218	0.4218	0.4912

*While June samples were not sterile filtered between the "init" and "start" steps, SM1 and SM2 samples were.

All samples except the Gooseberry River base flow sample show an increase in microbial abundance for "exp" and "control" samples compared to their respective "start" sample. Seasonal variation in responses of bacterial growth is also noted. Snow melt "exp" samples all show a higher microbial abundance than "control" samples. In contrast, base flow samples all show a higher microbial abundance in "control" samples than "exp" samples. While an unintended consequence of the experimental design, this seasonal variation indicates in interesting feedback between irradiated snow melt DOM and microbial growth; perhaps the snow melt DOM is acting as a better sunscreen or food source for the microbial community present in the samples.

3.5. Microbial Degradation

Microbial degradation treatments were analyzed using June 2010 base flow samples inoculated with unfiltered Lake Superior water ("LS WHOLE"). All results other than the undiluted inoculant ("LS Whole") in Tables 16 and 17 are the average of replicate samples.

Table 16. The e2/e3 values of all samples before (start) and after (end) microbial incubations. Values in parentheses are average deviations of replicate samples (n=2).

	Gb-June	F-June	Am-June	K-June	M-June
LS WHOLE	5.68 (0.5)	5.68 (0.5)	5.68 (0.5)	5.68 (0.5)	5.68 (0.5)
start control	4.84 (0.03)	5.01 (0.02)	5.48 (0.0001)	4.66 (0.02)	5.67 (0.05)
start innoc	4.58 (0.09)	5.00 (0.00)	5.49 (0.007)	4.50 (0.02)	5.51 (0.01)
end control	5.11 (0.02)	5.07 (0.03)	5.48 (0.03)	5.00 (0.02)	5.55 (0.05)
end innoc	5.13 (0.02)	5.12 (0.03)	5.48 (0.07)	4.99 (0.02)	5.64 (0.08)

Table 17. Organic carbon analysis (in mg/L) of samples before (start) and after (end) microbial incubations. Values in parentheses are the standard deviation of replicate samples (n=3).

	Gb-June	F-June	Am-June	K-June	M-June
LS WHOLE	2.06 (0.04)	2.06 (0.04)	2.06 (0.04)	2.06 (0.04)	2.06 (0.04)
start control	22.5 (0.4)	14.4 (0.3)	11.4 (0.2)	14.6 (0.3)	11.1 (0.1)
start innoc	23.4 (0.2)	15.8 (0.2)	12.2 (0.2)	14.9 (0.3)	12.7 (0.2)
end control	20.6 (0.4)	13.9 (0.1)	12.0 (0.7)	13.3 (0.2)	10.9 (0.1)
end innoc	20.7 (0.3)	14.54 (0.09)	12.5 (0.3)	13.7 (0.4)	11.0 (0.1)

Control samples did not show a significant difference in organic carbon concentration between “start” and “end” samples following microbial incubations ($p=0.4$, two sample t-test assuming equal variance, $t=0.241$). Similarly, inoculated samples did not show a significant difference between “start” and “end” ($p=0.3$, two sample t-test assuming equal variance, $t=0.495$). All samples except June Amity Creek showed a decrease in the OC concentration from “start control” to “end control” and from “start innoc” to “end innoc”.

Inoculated samples from the microbial degradations treatment show a more substantial decrease in OC concentration relative the decrease in OC concentration from “exp” samples in photodegradation treatments. Similar levels of change are shown in e2/e3 values for the microbial degradation treatment relative to the photodegradation treatment.

Future work in microbial degradations can be analyzed in detail by ensuring that “init” samples are filtered to remove all microbes, beginning the microbial degradation treatments without an intermediate refrigerator storage period, and perhaps also including a poisoned control. This will provide “innoc” samples that are inoculated with only the intended “LS WHOLE” inoculants, and “control” samples that are not exposed to microbial degradation.

4. Conclusions

One component of dissolved organic matter, the colored dissolved organic matter, significantly affects the light penetration in lake waters and it has the potential to affect light quality on longer temporal and larger spatial scales than suspended sediments do because colored dissolved organic matter does not settle out of a water column. Information from previously conducted studies shows that light exposure alters composition and bioavailability of dissolved organic matter (e.g. Biddanda and Cotner, 2003), and that tributaries are important sources of colored dissolved organic matter input into Lake Superior (e.g., Minor and Stephens, 2008).

Table 18. Results of this study to determine the role of watershed urbanization and season on the input and fate of photodegraded DOM.

	Relative Importance	**Description**
Seasonal effects	+++	Very strong impact
Watershed Urbanization	+	Some impact
$SUVA_{254}$	++	Most irradiated samples showed loss of aromaticity.
e2/e3	+++	All irradiated samples showed a reduction in molecular size.
OC concentration	+	Most irradiated samples showed a loss of OC.

The goals of this study were to compare the roles of watershed urbanization and season on photodegradation and input of dissolved organic matter into Lake Superior. Irradiated samples were often found to show a loss in specific UV-absorption, indicating a loss in aromaticity, especially in areas of rural land use. Irradiated samples from all sampling times showed an increase in the ratio of absorbance at 250 nm to absorbance at 365 nm, indicating a decrease in molecular size. During the early base flow season (and to some extent during the later summer), irradiated samples showed statistically significant decreases in the concentration of dissolved organic carbon relative to control samples. During snow melt, dissolved organic carbon changes were much smaller, more scattered in sign and often within precision of measurement and/or similar in range to those of control samples. These results show that season has a stronger impact on the photoloss of dissolved organic carbon than sample location. As a result, the effects of land use in stream catchments should be analyzed across seasons to determine the impact on the input and reactivity of dissolved organic matter in coastal aquatic systems.

5. References

Amado, A. M., V. C. Farjalla, F. A. Esteves, R. L. Bozelli, F. Roland, and A. Enrich-Prast, 2006. Complementary pathways of dissolved organic carbon removal pathways in clear-water Amazonian ecosystems: photochemical degradation and bacterial uptake. FEMS Microbiol Ecol. 56: 8-17.

Amon, R.M.W. and R. Benner, 1996. Bacterial utilization of dissolved organic matter. Limnol. Oceanogr. 41(1), 41-51.

Anesio, A.M., W. Granéli, G. R. Aiken, D. J. Kieber, and K. Mopper, 2005. Effect of humic substance photodegradation on bacterial growth and respiration in lake water. App. Env. Mircrobiol. 71(10), 6267-6275.

Arrigo, K., 1994. Impact of ozone depletion on phytoplankton growth in the Southern Ocean: large-scale spatial and temporal variability. Mar. Ecol. Prog. Ser. 114: 1-12.

Barnes, R. T., and P. A. Raymond, 2009. The contribution of agricultural and urban activities to inorganic carbon fluxes within temperate watersheds. Chem. Geo. 266, 318-327.

Benner, R. and B. Biddanda, 1998. Photochemical transformations of surface and deep marine dissolved organic matter: effects on bacterial growth. Limnol. Oceanogr. 43, 1373-1378.

Biddanda, B.A. and J.B. Cotner, 2003. Enhancement of dissolved organic matter bioavailability by sunlight and its role in the carbon cycle of Lakes Superior and Michigan. J. Great Lakes Res. 29(2), 228-241.

Bracchini L., S. Loiselle, A. M. Dattilo, S. Mazzuoli, A. Co´zar, and C. Rossi, 2004. The spatial distribution of optical properties in the ultraviolet and visible in an aquatic ecosystem. Photochem. and Photobiol. 80: 139-149.

Bushaw, K.L., R. G. Zepp, M. A. Tarr, D. Schulz-Janders, R. A. Bourbonniere, R. E. Hodson, W. L. Miller, D. A. Bronk, and M. A. Moran, 1996. Photochemical release of biologically available nitrogen from dissolved organic matter. Nature, 381(6581), 404-407.

Chin, W. C., M.V. Orellana and P. Verdugo., 1998. Spontaneous assembly of marine dissolved organic matter into gels. Nature. 391, 568-572.

Dalzell, B. J., E. C. Minor, and K. M. Mopper, 2009. Photodegradation of estuarine dissolved organic matter: a multi-method assessment of DOM transformation. Org. Geochem. 40, 243-257.

Del Vecchio, R. and N.V. Blough, 2002. Photobleaching of chromophoric dissolved organic matter in natural waters: kinetics and modeling. Mar. Chem. 78(4), 231-253.

Feng, X., L. L. Nielsen, and M. J. Simpson, 2007. Responses of soil organic matter and microorganisms to freeze-thaw cycles. Soil. Biol. Biochem. 39(8), 2027-2037.

Francko, D.A. and R.T. Heath, 1979. Functionally distinct classes of complex phosphorus compounds in lake water. Limnol. Oceanogr. 24, 463-473.

Goodman, K. J., M. A. Baker, and W. A. Wurtsbaugh, 2011. Lakes as buffers of stream dissolved organic matter (DOM) variability: Temporal patterns of DOM characteristics in mountain stream-lake systems. Journal of Geophysical Research. 116 (G00N02), 1-15.

Granéli, W., M. Lindell and L. Tranvik, 1996. Photo-oxidative production of dissolved inorganic carbon in lakes of different humic content. Limnol. Oceanogr. 41(4): 698–706.

Green, S.A. and N.V. Blough, 1994. Optical absorption and fluorescence properties of chromophoric dissolved organic matter in natural waters. Limnol. Oceanogr. 39(8), 1903-1916.

Harris, D. C., 2007. Propagation of Uncertainty from Random Error. Quantitative Chemical Analysis Seventh Edition, 44-46.

Hedges, J.I., 1992. Global biogeochemical cycles: Progress and problems. Mar. Chem. 39, 67-93.

Hieb, W.S., 2005. Identifying the sources of fecal coliform bacteria in Lake Superior watersheds. University of Minnesota. M.S. Thesis, Water Resources Science.

Hiriart-Baer, V.P. and R.E.H. Smith, 2005. The effect of ultraviolet radiation on freshwater planktonic primary production: the role of recovery and mixing processes. Limnol. Oceanogr. 50(5), 1352-1361.

Kaiser, E. and B. Sulzberger, 2004. Phototransformation of riverine dissolved organic matter (DOM) in the presence of abundant iron: Effect on DOM bioavailability. Limnol. Oceanogr. 49(2), 540-554.

Kieber, D.J., and K. Mopper, 1987. Photochemical formation of glyoxylic and pyruvic acids in seawater. Mar. Chem. 21, 135-149.

Köhler, S., I. Buffam, A. Jonsson, and K. Bishop, 2002. Photochemical and microbial processing of stream and soil water dissolved organic matter in a boreal forested catchment in northern Sweden. Aquat. Sci. 64, 269-281.

Kujawinski, E. B., R. Del Vecchio, N. V. Blough, G. C. Klein, and A. G. Marshall, 2004. Probing molecular-level transformations of dissolved organic matter: insights on photochemical degradation and protozoan modifications of DOM from electrospray ionization Fourier transform ion cyclotron resonance mass spectrometry. Mar. Chem. 92, 23-37.

Lakesuperiorstreams, 2009. LakeSuperiorStreams: Community Partnerships For Understanding Water Quality and Stormwater Impacts at the Head of the Great Lakes (http://lakesuperiorstreams.org).

Larson, J.H., P. C. Frost, D. M. Lodge, and G. A. Lamberti, 2007. Photodegradation of dissolved organic matter in forested streams in the northern Great Lakes region. J. N. Am. Benthol. Soc. 26(3), 416-425.

Macdonald, R., D. Mackay, and B. Hickie, 2002. Contaminant amplification in the environment. Environmental Science and Technology. 36, 457A-462A.

Meyer, T., and F. Wania, 2008. Organic contaminant amplification during snowmelt. Water Research. 42: 1847-1865.

Meyer T., Y.D. Lei, and F. Wania, 2011. Transport of polycyclic aromatic hydrocarbons and pesticides during snowmelt within an urban watershed. Water Research, 45(3), 1147-1156.

Minnesota Department of Natural Resources, 2011. "Trout stream and trout lake designation request." Fwd. by Neil Vanderbosch. E-mail to the author. 6 June 2011.

Minor, E. C., B. J. Dalzell, A. Stubbins, and K. Mopper, 2007. Evaluating the photoalteration of estuarine dissolved organic matter using direct temperature-resolved mass spectrometry and UV-visible spectroscopy. Aquat. Sci. 69, 440-455.

Molot, L. A. and P. J. Dillon, 1997. Photolytic regulation of dissolved organic carbon in northern lakes. Global Biogeochemical Cycles. 11(3): 357–365.

Moran, M. A. and R. E. Hodson, 1990. Bacterial production on humic and nonhumic components of dissolved organic carbon. Limnol. Oceanogr. 35(8), 1744-1756.

Moran, M. A. and R. G. Zepp, 1997. Role of photoreactions in the formation of biologically labile compounds from dissolved organic matter. Limnol. Oceanogr. 42(6), 1307-1316.

Moran, M. A., W. M. Sheldon, and R. G. Zepp, 2000. Carbon loss and optical property changes during long-term photochemical and biological degradation of estuarine dissolved organic matter. Limnol. Oceanogr. 45(6), 1254-1264.

Morris, D. P., and B. R. Hargreaves, 1997. The role of photochemical degradation of dissolved organic carbon in regulating the UV transparency of three lakes on the Pocono Plateau. Limnol. Oceanogr. 42:239– 249.

Obernosterer, I. and R. Benner, 2004. Competition between biological and photochemical processes in the mineralization of dissolved organic carbon. Limnol. Oceanogr. 49(1), 117-124.

Obernosterer, I., B. Reitner, and G. J. Herndl, 1999. Contrasting effects of solar radiation on dissolved organic matter and its bioavailability to marine bacterioplankton. Limnol. Oceanogr. 44, 1645-1654.

Petrone, K. C., 2010. Catchment export of carbon, nitrogen, and phosphorus across an agro-urban land use gradient, Swan-Canning River system, southwestern Australia. Journal of Geophysical Research. 115 (G01016), 1-16.

Peuravuori, J. and K. Pihlaja, 1997. Molecular size distribution and spectroscopic properties of aquatic humic substances. Analytica Chimica Acta. 337 (2), 122-149.

Reche, I., E. Pulido-Villena, J. M. Conde-Porcuna, and P. Carrillo, 2001. Photoreactivity of dissolved organic matter from high-mountain lakes of Sierra Nevada, Spain. Arctic, Antarctic, and Alpine Research 33, 426–434.

Schlesinger, W.H., 1997. Biogeochemistry: An analysis of global change. *Academic Press*, San Diego, CA.

Sulzberger, B. and E. Durisch-Kaiser, 2009. Chemical characterization of dissolved organic matter (DOM): A prerequisite for understanding UV-induced changes of DOM absorption properties and bioavailability. Aquat. Sci. 71, 104-126.

Tranvik, L. J. and S. Bertilsson, 2001. Contrasting effects of solar UV radiation on dissolved organic sources for bacterial growth. Ecol. Letters. 4, 458-463.

Uyguner, C. S. U., and M. Bekbolet, 2005. Implementation of spectroscopic parameters for practical monitoring of natural organic matter. Desalination. 176, 47-55.

Vähätalo, A.V., K. Salonen, U. Münster, M. Järvinen, and R. G. Wetzel, 2003. Photochemical transformation of allochthonous organic matter provides bioavailable nutrients in a humic lake. Arch. Hydrobiol. 156(3), 287-314.

Vähätalo, A.V. and Wetzel, R.G., 2008. Long-term photochemical and microbial decomposition of wetland-derived dissolved organic matter with alteration of ^{13}C:^{12}C mass ratio. Limnol. Oceanogr. 53(4), 1387-1392.

Vander Zanden, M. J. and C. Gratton, 2011. Blowin' in the wind: reciprocal airborne carbon fluxes between lakes and land. Can. J. of Fish Aquat. Sci. 68(1), 170-182.

Vodacek, A. N., N. V. Blough, M. D. DeGrandpre, E. T. Peltzer, and R. K. Nelson, 1997. Seasonal variation of CDOM and DOC in the *Middle Atlantic* Bight: Terrestrial inputs and photooxidation. Limnol. Oceanogr. 42(4), 674-686.

Wang, L, J. Lyons, P. Kanehi, R. Bannerman, and E. Emmons, 2000. Watershed urbanization and changes in fish communities in southeastern Wisconsin streams. J. Am. Water Resources Association. 36(5), 1173-1189.

Wania, F., 1999. On the origin of elevated levels of persistent chemicals in the environment. Environ. Sci. Pollut. Res. 6(1), 11-19.

Weishaar, J.L., G.R. Aiken, B.A. Bergamaschi, M.S. Fram, R. Fugii, and K. Mopper, 2003. Evaluation of specific ultraviolet absorbance as an indicator of the chemical composition and reactivity of dissolved organic carbon. Environ. Sci. Technol. 37, 4702-4708.

Wetzel, R. G., P. G. Hatcher, and T. S. Bianchi, 1995. Natural photolysis of recalcitrant dissolved organic matter to simple substrates for rapid bacterial metabolism. Limnol. Oceanogr. 40, 1369-1380.

Wohlers, J., A. Engel, E. Zöllner, P. Breithaupt, K. Jürgens, H.-G. Hoppe, U. Sommer, and U. Riebesell, 2009. Changes in biogenic carbon flow in response to sea surface warming. PNAS. 106(17). 7067-7072.

Wu, F. C., R. B. Mills, Y. R. Cai, R. D. Evans, and P. J. Dillon, 2005. Photodegradation-induced changes in dissolved organic matter in acidic waters. Can. J. Fish. Aquat. Sci. 62, 1019-1027.

Zepp, R. G., D. J. Erickson III, N. D. Paul, and B. Sulzberger, 2011. Effects of solar UV radiation and climate change on biogeochemical cycling: interactions and feedbacks. Photochem. Photobiol. 10, 261-279.